Task No. NR 387-022
ONR Contract No.: 1202(07)

WATER TECHNICAL REPORT NO. 31

REMOTE SENSING BY INFRARED AND MICROWAVE RADIOMETRY

I. BASIC PRINCIPLES
II. A TECHNIQUE FOR THE CORRECTION OF AIRBORNE MEASUREMENTS OF APPARENT SURFACE TEMPERATURE OF NATURAL WATER BODIES
III. POTENTIAL APPLICATIONS OF INFRARED AND MICROWAVE RADIOMETRY

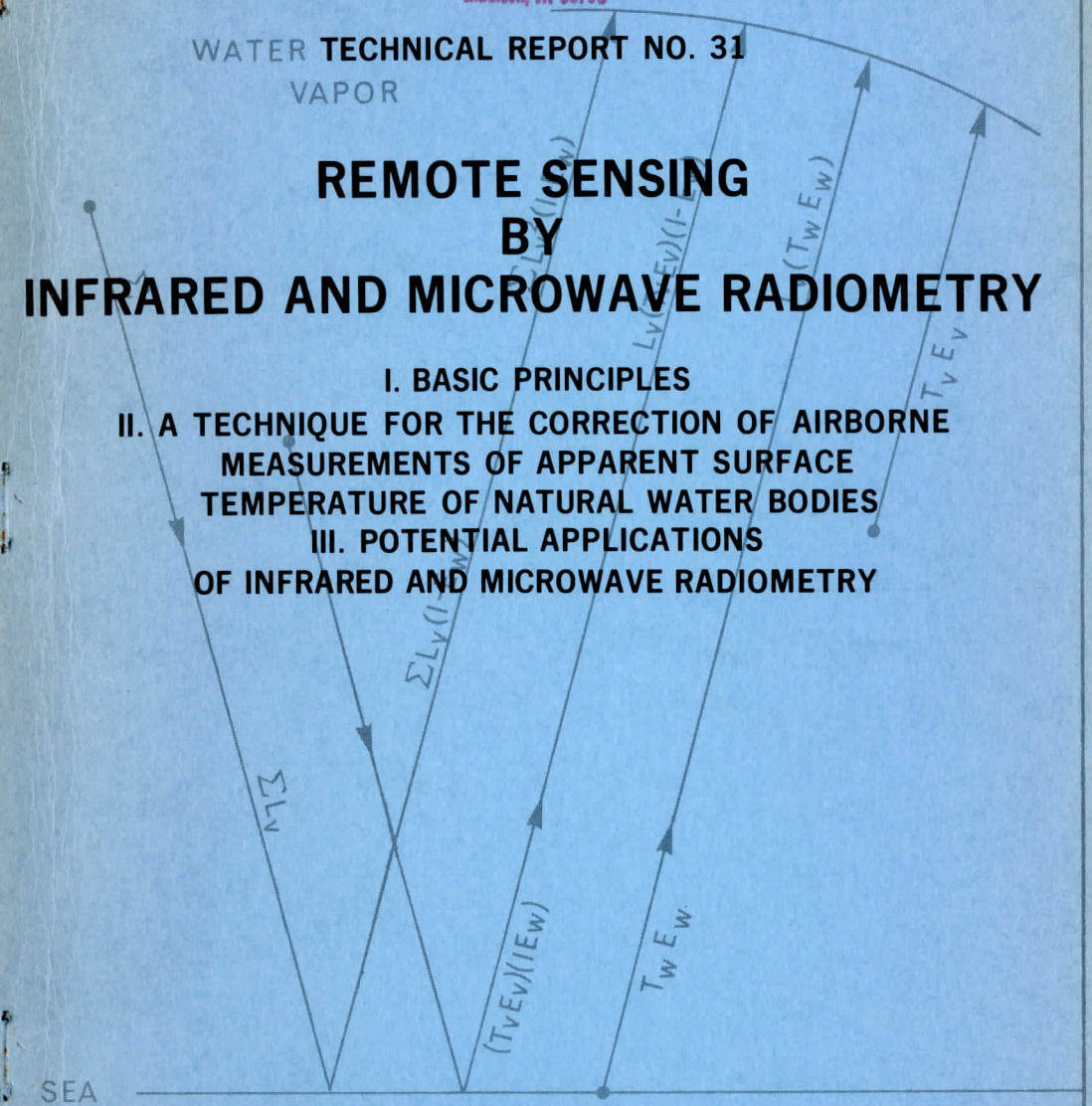

The University of Wisconsin
Department of Meteorology
Madison, Wisconsin 53706

February 1967

REMOTE SENSING
BY
INFRARED AND MICROWAVE RADIOMETRY

I. BASIC PRINCIPLES
II. A TECHNIQUE FOR THE CORRECTION OF AIRBORNE MEASUREMENTS OF APPARENT SURFACE TEMPERATURE OF NATURAL WATER BODIES
III. POTENTIAL APPLICATIONS OF INFRARED AND MICROWAVE RADIOMETRY

by
VELAYUDH KRISHNA MENON
AND
ROBERT A. RAGOTZKIE

Technical Report No. 31

Task No. NR 387-022 ONR Contract No.: 1202(07)

The research reported in this document has been sponsored by the Geography Branch of the United States Office of Naval Research.

The University of Wisconsin
Department of Meteorology
Madison, Wisconsin 53706
February 1967

200-125

TABLE OF CONTENTS

LIST OF FIGURES

Part I. BASIC PRINCIPLES

I. INTRODUCTION

Remote sensing by passive techniques in the visible region, as in photography),has been known for over a century. The use of the infrared region of the electromagnetic spectrum for the same purpose is fairly recent, but is well established by now. The far infrared or the microwave region has been under theoretical investigation more recently and results so far indicate possibilities superior to the other regions for some purposes.

Passive microwave technology is a sort of hybrid between radar and infrared. It has the same theoretical basis as in infrared, but the instrumentation is more akin to radar. In many important applications of remote sensing such as snow and cloud measurements, it augments infrared measurements. Water vapor and carbon dioxide have strong absorption bands at 1.25 cm and 5 mm respectively, and hence measurements in these wave-lengths can provide excellent information about their absorption spectrum in the atmosphere. The chief advantages of the microwave region over the visible and the infrared regions are:

(1) The propagation problems under various atmospheric conditions is considerably less serious. At a wavelength of 1.8 cm, there is practically no atmospheric interference.

(2) Microwave radiations originate from beneath the surface and hence instead of skin temperature, the body temperature may be obtained.

(3) Compared to active techniques like radar, measurements are easier and more direct.

II. THEORY

Any material whose temperature is above 0 °K is a source of radiation. This originates from the thermal agitation of its molecules. In solids and liquids, because of the physical constraints put upon them, the molecules are unable to radiate in their characteristic manner. The result is a continuous emission and absorption spectra over a wide range of wave-lengths without sharp discontinuities. This thermal radiation is characteristic of the temperature of the substance rather than of the substance itself. Hence, by a reverse process, from an examination of the radiations from a material, it should be possible to make a reasonable inference of its temperature. Passive remote sensing devices operating at suitable wave-length regions can be used to detect this thermal energy and convert it into corresponding radiometric temperatures.

A. Reception of Thermal Radiation. A perfect thermal radiator is one that emits for a given temperature the greatest power per unit

surface area, as in a black-body. This can be expressed as

$$W = \frac{dp}{da} \tag{1}$$

where W, the total radiant power per unit surface area is called the emittance and this is a maximum for a black-body.

This radiation is essentially a wide band random noise signal, whose intensity is given by Planck's radiation law,

$$W = \frac{2\pi hc}{\lambda^3} \cdot \frac{1}{\exp\left[\frac{hc}{K\lambda T}\right] - 1} \tag{2}$$

where:

W = power per unit bandwidth per unit area of the source in watts per meter^2 cps.

h = Planck's constant, 6.63×10^{-34} joule-sec.

c = velocity of light, 3×10^8 meters sec^{-1}.

k = the Stefan-Boltzman constant, 1.33×10^{-23} joules per deg Kelvin.

λ = the wavelength in meters.

T = temperature in °K.

This equation is plotted in Fig. (1) for various temperatures (Collins Research Report, 1961).

In the microwave region, where the wavelength is of the order of a few centimeters

$$k\lambda T >> hC$$

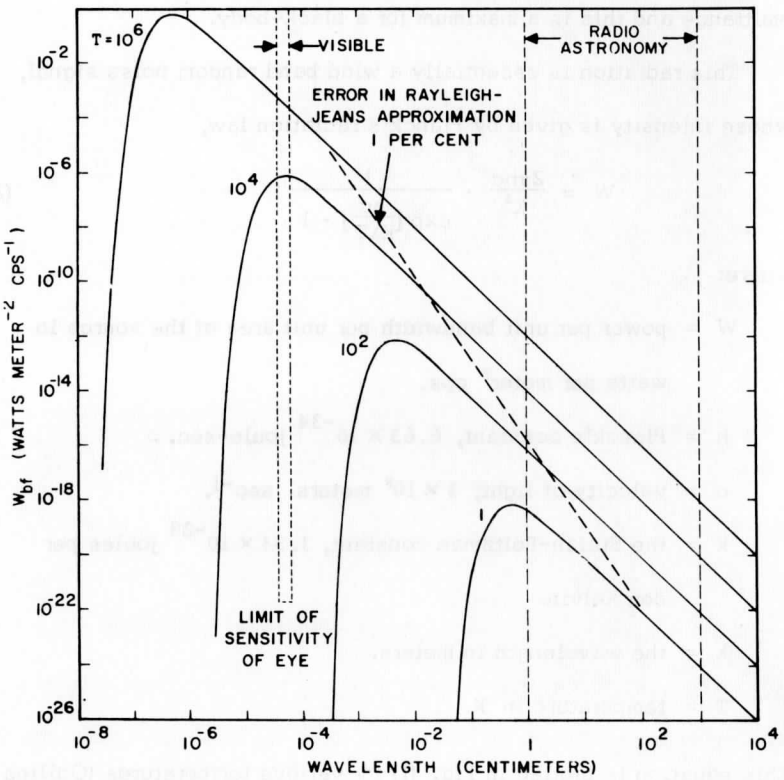

Figure 1. Blackbody Radiant Emittance Per Unit Bandwidth.

so that the Rayleigh-Jean's approximation can be used to represent the radiation intensity with an error of less than one percent, and

$$W = \frac{2\pi KT}{\lambda^2} \tag{3}$$

As can be seen from Fig. (1), the energy in the microwave region is less than that available in the infrared region by several orders of magnitude. However, in the microwave region, the sensors can be made with a much higher sensitivity than is presently possible in the infrared region. In fact, these two factors approximately compensate to allow equivalent operations in the infrared and microwave spectrum (Conway, 1964).

B. Apparent Blackbody Temperature. If the radiating object is not a perfect blackbody, its temperature is represented as an "apparent temperature." This is defined as the temperature at which a blackbody would radiate the same amount of energy. Evidently, the apparent temperature is related to the actual temperature by the emissivity, ϵ, of the object. Also, a non-blackbody will reflect a portion of the radiation incident upon it, the amount depending upon the reflectance $1-\epsilon$. Thus the total apparent blackbody temperature is given by

$$Tb' = \epsilon T + (1-\epsilon)Te \tag{4}$$

where Te is the incident radiation temperature, which is representative of the environment of the surface. This is the temperature that

is observed by a microwave radiometer. In the infrared range, however, because of the shorter wavelengths involved, the Rayleigh-Jean approximation is not applicable and therefore the apparent temperature is given by

$$Tb'^4 = \epsilon T^4 + (1-\epsilon)Te^4 \tag{5}$$

the effect of the propagation medium being neglected for the time being. This shows that the infrared is very much more sensitive to changes in emissivity. For example, a monomolecular layer of oil on the water surface may cause sizable changes in the apparent infrared temperature measured.

The power received by a lossless microwave antenna having a single narrow lobe directional pattern is given by

$$W = K\, Tb'\, \Delta f \tag{6}$$

where Δf is the bandwidth of the system and K an instrument constant. Therefore, in terms of the temperature and emissivity of the radiating object,

$$W = K\Delta f[\epsilon T + (1-\epsilon)Te]. \tag{7}$$

An equivalent expression for power received by an infrared radiometer can be written in the form

$$W = K'\, E(W_r - W_t) \tag{8}$$

where K' is an instrument constant, E is the efficiency of the filter system, and $(W_r - W_t)$ is the difference in flux emitted by the radiometer and target.

This means that in spite of the larger power available in the infrared region, the increased attenuation by the atmospheric constituents and the low efficiency of the filter system (Fig. (2)) combine to reduce the infrared capabilities (Berberian, 1964).

III. PROBLEM OF EMISSIVITY

A rough or diffuse surface will emit only a fraction of the radiation emitted by a blackbody at the same temperature. This fraction is called the surface emissivity. As shown in Fig. (3-a), the surface will reflect a certain fraction, ρ_λ, and absorb a fraction α_λ. Conservation of energy requires

$$\rho_\lambda + \alpha_\lambda = 1 \tag{9}$$

In the case of a semi-transparent slab, a fraction τ_λ is transmitted as shown in Fig. (3-b). Hence

$$\tau_\lambda + \rho_\lambda + \alpha_\lambda = 1 \tag{10}$$

Here $\alpha_\lambda = \epsilon_\lambda$ is called the body emissivity. Its value depends on slab thickness.

Emission of real surface. A real surface does not emit or absorb like a blackbody. Hence ϵ_λ and α_λ are always less than unity and ρ_λ is always finite as opposed to zero for a blackbody. These three parameters behave in a complex manner for natural surfaces, being functions of wavelength, angle of emission, nature of surface,

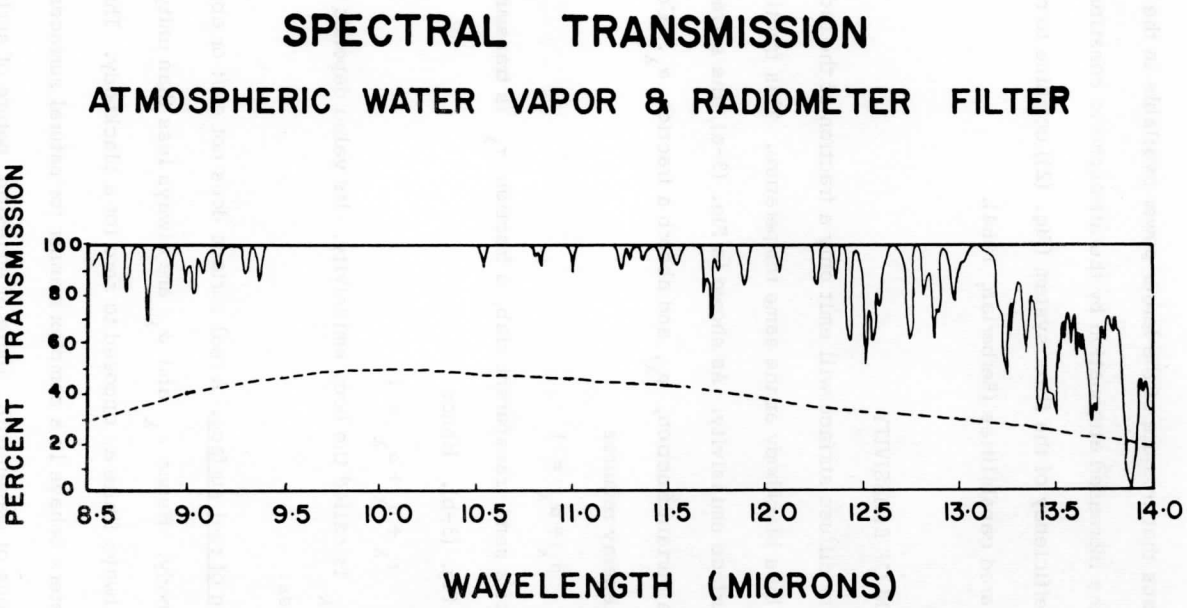

Figure 2. Spectral Transmission, Atmospheric Water Vapor and Radiometer Filter.

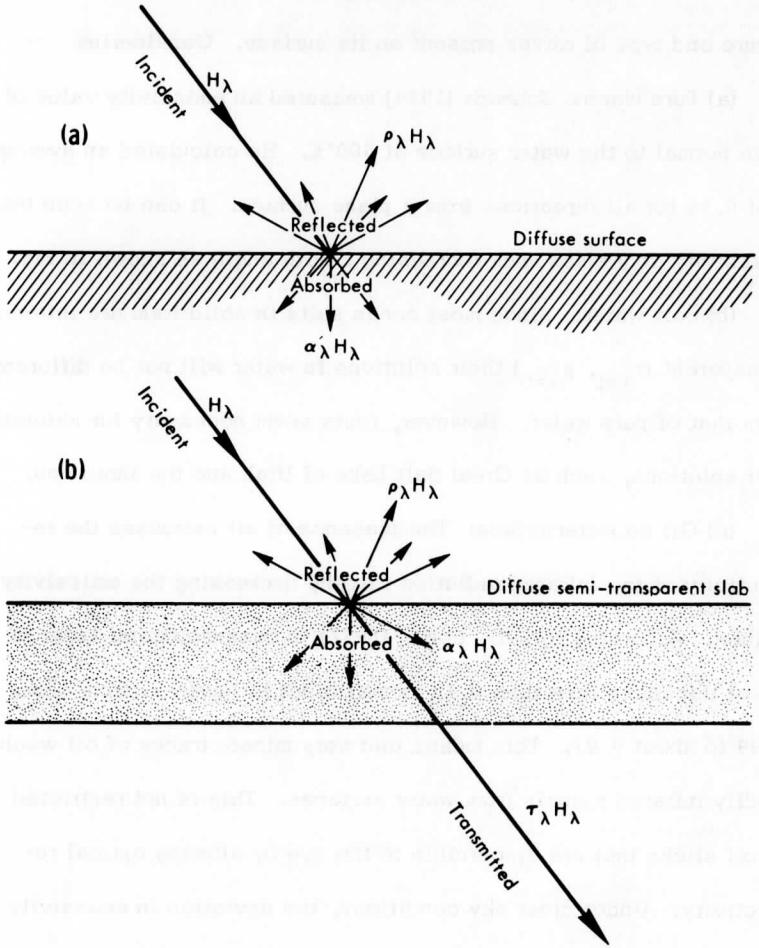

Figure 3. Schematic diagram showing the behavior of a beam of spectral irradiance H incident on (a) a diffuse surface, or (b) a semi-transparent slab.

etc. As for water, its radiant characteristics change also with the nature and type of waves present on its surface. Considering

(a) Pure water: Schmidt (1934) measured an emissivity value of 0.96 normal to the water surface at 300°K. He calculated an average ϵ of 0.90 for all directions from a plane surface. It can be seen that emissivity decreases with increasing zenith angle as shown in Fig. (4).

(b) Salt water: Since most ocean salts in solid form are infrared transparent ($\tau_{\lambda=1}$, $\rho_{\lambda=0}$) their solutions in water will not be different from that of pure water. However, tests seem necessary for saturated salt solutions, such as Great Salt Lake of Utah and the Dead Sea.

(c) Oil on water surface: The presence of oil increases the reflectivity of the infrared radiation thereby decreasing the emissivity values. According to Bell, et al. (1957), a monomolecular layer of oil of thickness less than 0.1μ is sufficient to lower ϵ from about 0.99 to about 0.97. This means that very minute traces of oil would modify infrared signals from water surfaces. This is not restricted to oil slicks that are discernible to the eye by altering optical reflectivity. Under clear sky conditions, the deviation in emissivity if neglected could cause surface temperature to read lower by more than 1°K, a serious error in oceanographic investigation. Garrett, et al. (1963) find measurable oil layers not only in coastal waters off Panama and New Jersey, but also east of Newfoundland. Not

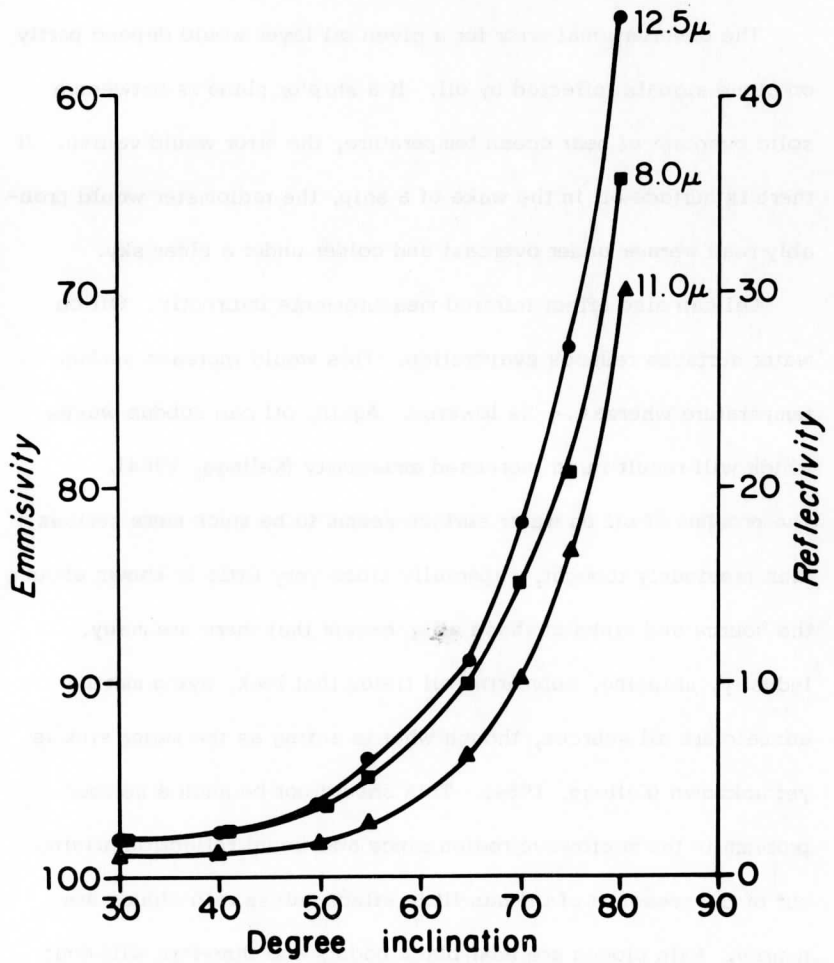

Figure 4. Reflectivity and emissivity of a smooth water surface as a function of inclination angle for three wavelengths (8.0, 11.0, and 12.5μ). After McSwain and Bernstein (1960)

much oil is necessary to provide these layers; a few hundred tons will suffice for Lake Michigan, for example (Buettner, 1964).

The observational error for a given oil layer would depend partly on cloud signals reflected by oil. If a ship or plane is between a solid overcast of near ocean temperature, the error would vanish. If there is surface oil in the wake of a ship, the radiometer would probably read warmer under overcast and colder under a clear sky.

Oil can also affect infrared measurements indirectly. Oil on water surfaces reduces evaporation. This would increase surface temperature whereas ϵ is lowered. Again, oil can subdue waves which will result in an increased emissivity (Kellogg, 1964). The problem of oil on water surface seems to be much more serious than previously thought, especially since very little is known about the source and sinks of these oils, except that there are many. Industry, shipping, submarine oil fields that leak, dying marine animals are all sources, though what is acting as the major sink is yet unknown (Kellogg, 1964). This should not be such a serious problem in the microwave region since additional reflection arising out of the presence of oil has little effect unless rain clouds are nearby. Rain clouds are near black bodies and therefore will emit some radiation in the microwave region. This can be reflected by the oil on water surface and sensed by the radiometer.

(d) The effect of waves: An agitated sea surface may be considered as consisting of many mirrors randomly arranged with respect to the zenith angle. For all wavelengths, reflectivity increases with increasing zenith angle ϕ, the increase becoming pronounced for ϕ greater than 60 degrees. An increasing amount of polarization also results.

The microwave region has a decided advantage over the infrared when the water surface is agitated. This is because, on an agitated water surface, the reflectivity is higher and this accounts for the emissivity being lower. In the wavelength region of 1.8 cm, the atmosphere is almost totally transparent (McAlister, 1965). Hence, any radiation that may reach the radiometer by reflection must originate from beyond the atmosphere. Even though this radiation from space cannot be completely excluded, for all practical purposes the space temperature can be taken to be near absolute zero. Therefore, the increased reflectivity will have no effect at this particular wavelength. On the other hand, for the infrared wavelengths, the atmospheric constituents like water vapor and carbon dioxide can emit in those wavelengths and at their respective temperatures. This may contribute to a decrease in the apparent temperature measured.

(e) Emissivity of non-homogeneous surface: Neglecting most land areas, which are highly nonhomogeneous by nature, it is pertinent

Table 1

EMISSIVITIES FOR THE 8--13μ AREA, MEASURED (PART 1) WITH BARNES IT-2 INFRARED THERMOMETER AND THE EMISSIVITY BOX. PART 2 (LITERATURE)

Material	ϵ_{IT}
1. Data by Clifford Kern, using emissivity box	
Quartz (agate)	0.712
Granite	.815
Feldspar	.870
Obsidian	.862
Basalt	.904
Dunite	.856
Granite, rough side	.898
Obsidian, rough side, broken glass appearance	.837
Basalt, rough side, shiny	.934
Dunite, rough side	.892
Silicon sandstone, polished side	.909
Silicon sandstone, rough side	.935
Dolomite, polished side $CaMg(CO_3)_2$	.929
Dolomite, rough side	.958
Dolomite gravel, 0.5 cm size rocks	.959
Plate silicon glass	.865
Parson's Black on Al sheet (no grooves)	.988
Plywood sheet	.962
Human skin	.980
Sand, quartz large grain	.914
Sand, quartz large grain wet with water (nearly saturated)	.936
Sand, Monterey, quartz small grain	.928
Concrete walkway, dry	.966
Asphalt paving	.956
Water, pure	.993
Water, plus thin film petroleum oil	.972
Water, plus thin film corn oil	.966
Water, covered by a thin sheet of polyethylene	.961
2. Data from other sources	
Melting snow	0.995
Ice	0.98
Vegetation	> 0.97
Gypsum	0.95
Sahara	0.8 - 0.9

Table 2

EFFECT OF SURFACE COVERINGS ON EXPECTED INCREASE (+) OR DECREASE (-) OF EMISSIVITY AND SURFACE TEMPERATURE

Surface	Nature of Surface	Disturbance	
		Day	Night
	8--13μ		
Smooth sea	Oil	- 0	- 0
	Oil (warm, dry weather)	- +	- +
	Steep waves	- -	- +
	Foam	0 -	0 -
	Snow on iceberg	+ -	+ -
	Ice on iceberg	- -	- -
Sand	Water	+ -	+ -
	Moist vegetation	+ -	+ -
	Dry vegetation	+ +	+ -
	Salt	- -	- ?
	Gypsum	+ -	+ ?
	Carbonates	+ 0	+ 0
	Horizontal rock	- -	- +
	Dust	+ +	+ -
	Steep valleys	+ +	+ -
	Cities	+ +	+ +
	Oases	+ -	+ +
Snow	All temperatures below $0^{\circ}C$		
	Rocks and sand	- +	- +
	Ice	- ?	- ?
	Crevasses	0 -	0 +
	All temperatures at or above $0^{\circ}C$		
	Rocks and sand	- +	- -
	Temperatures $\geq 0^{\circ}C$ day, $\leq 0^{\circ}C$ night		
	Crevasses	0 0	0 +
	Open leads, Arctic Ocean, winter and spring	0 +	0 +
	Microwave (1 cm)		
Sea	Iceberg	+ -	
	Foam	+ -	
	Waves	- 0	
	Cloud	+ -	
	Rain	+ -	
Snowfields	Melting	+ +	
	Rocks and sand	0 0	
Arctic Ocean ice (winter)	Open leads	- +	
	Snow over ice	0 -	

to ask how the emissivity of a surface such as water, extensive sand areas and large snow fields are modified when natural intrusions occur. Tables 1 and 2 from Clifford-Kern give emissivities under laboratory conditions for various materials and the effect of covering them with other natural substances (Kellogg, 1964).

IV. PROBLEM OF TRANSMISSION THROUGH ATMOSPHERE

All atmospheric gases except nitrogen and the noble gases absorb infrared radiation and microwave to some extent. In addition, clouds, haze and dust absorb and scatter thermal radiation. It follows from Kirchoff's Law that the atmosphere must also emit some thermal radiation. The absorption spectra for various atmospheric constituents on a clear day is shown in Fig. (5). In the infrared region most of the absorption can be attributed to water vapor, carbon dioxide and the 9.6μ absorption band of ozone. There is a weak oxygen band near 0.8μ. The 8 to 12μ infrared window is quite transparent except for the wings of the main bands.

The microwave region is affected by:

(a) Resonant absorption by gases such as water vapor, oxygen and ozone.

(b) Nonresonant absorption and scattering by clouds or precipitation. In the spectral region most pertinent to oceanographic work (6mm to 10cm), a choice of proper wavelengths can reduce the at-

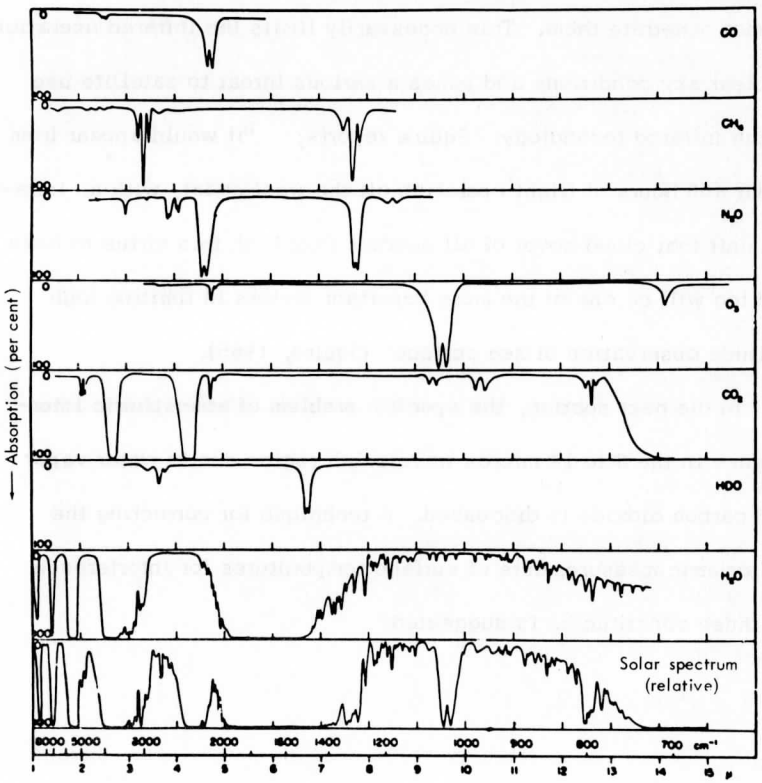

Figure 5. The near infrared solar spectrum, and absorption spectra of certain gases known to be in the atmosphere (Shaw, 1954).

mospheric influence to a workable minimum (Staelin, D. H., 1965).

Scattering by clouds and haze: For clouds thick enough to prevent direct passage of visible light, the combined action of scattering and absorption are so great that the infrared radiation simply cannot penetrate them. This necessarily limits the infrared operation to clear sky conditions and poses a serious threat to satellite use of the infrared technology. Squire reports, "it would appear from about 400 hours of flight operation off the west coast, with an infrared unit that cloud cover of all degrees from high thin cirrus to haze and fog will be one of the more important factors in limiting high altitude observation of sea surface" (Squire, 1965).

In the next section, the specific problem of atmospheric interference in the 8 to 14 micron wavelength region due to water vapor and carbon dioxide is discussed. A technique for correcting the radiometric measurements of surface temperatures for interference by these constituents is suggested.

PART II. A METHOD FOR THE CORRECTION OF AIRBORNE MEASUREMENTS OF SURFACE TEMPERATURES OF NATURAL WATER BODIES

I. INTRODUCTION

Infrared radiometers sensitive to various parts of the electromagnetic spectrum have become a common tool in the hands of geophysicists, space scientists, oceanographers, and others. An instrument of this type which senses radiation in the wavelength region of 8 to 13.5 microns is now frequently used for surface temperature measurements of natural water bodies. The instrument is usually carried aloft in an aircraft and flown at altitudes ranging from 500 feet to 1500 feet although it is also being used from surface vessels for air-sea interface studies.

The instrument has the singular advantage that it operates in a part of the electromagnetic spectrum known as the atmospheric water vapor window (Fig. (6)) of wavelength 8 to 13.5 microns. This means that it can exploit a spectral region in which the atmosphere is highly transparent and at the same time make use of the peak region of the terrestrial blackbody emission (Fig. (7)).

When the instrument is used under humid conditions, the absorption of radiation in the "wings of the window" can cause significant errors in the estimation of the target temperature. The object of the present study is to examine the effects of the pertinent atmos-

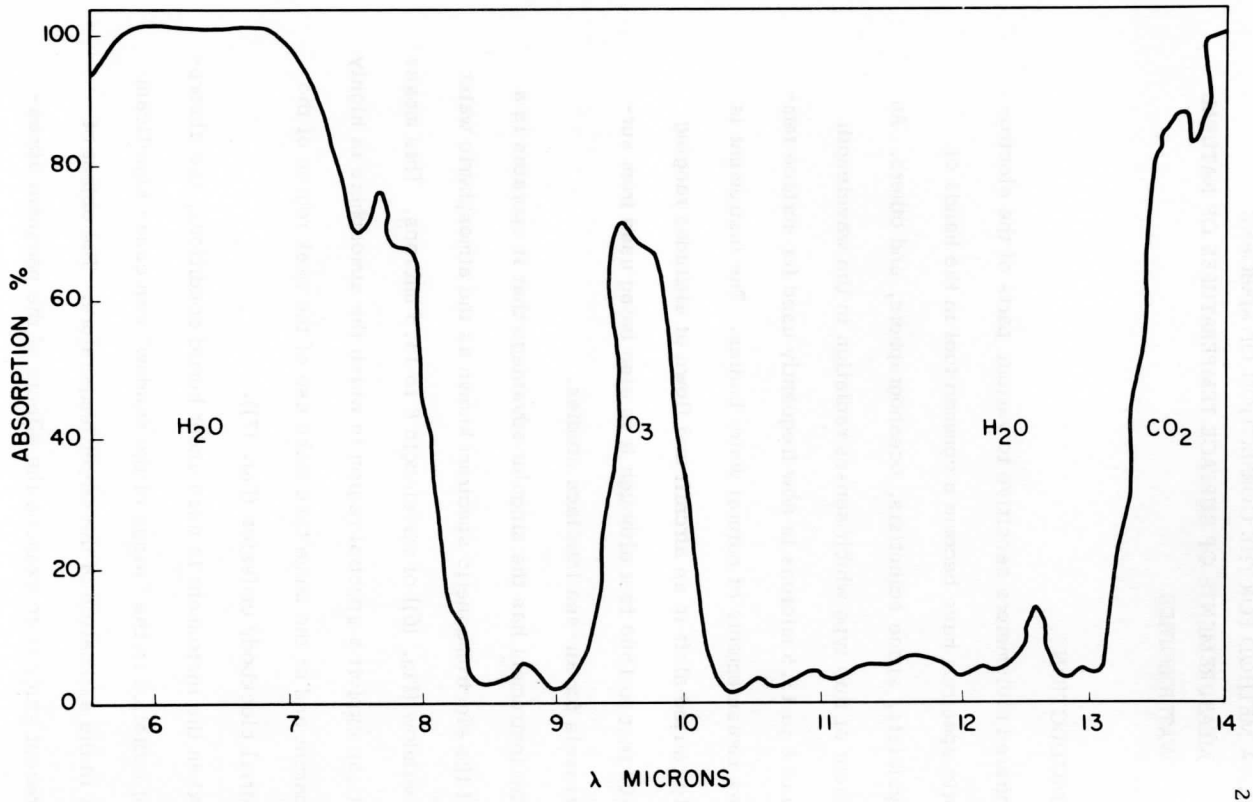

Figure 6. Absorption by the atmosphere between 5.3 and 14 μ (after Adel). There were 2.1 mm of precipitable water present for the observations below 11 μ and 1.3 mm above 11 μ. (Hess p. 119).

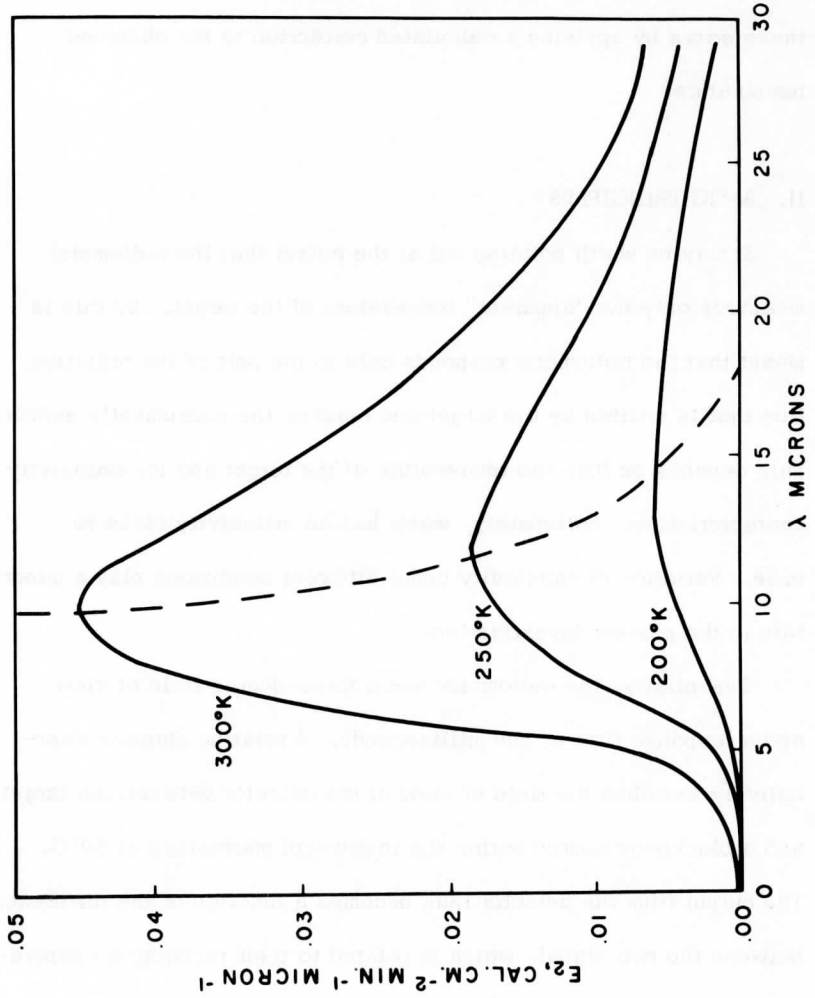

Figure 7. Selected blackbody radiation curves. The dashed line connects the points of maximum radiation of each curve (after Hess, pp. 125).

pheric constituents water vapor and carbon dioxide on the apparent surface temperatures measured by the radiometer and to minimize these errors by applying a calculated correction to the observed temperature.

II. BASIC PRINCIPLES

It may be worth pointing out at the outset that the radiometer measures only the "apparent" temperature of the target. By this is meant that the radiometer responds only to the part of the radiative flux that is emitted by the target and reaches the instrument's sensor. This depends on both the temperature of the target and its emissivity characteristics. Fortunately, water has an emissivity close to 0.98. Variation of emissivity under different conditions play a minor role in the present investigation.

Essentially, the radiometer has a three-degree field of view and a response time of 500 milliseconds. A rotating chopper alternatively switches the field of view of the detector between the target and a blackbody source within the instrument maintained at 50°C. The output from the detector thus becomes a function of the difference between the two signals which is related to their respective temperatures according to Stefan-Boltzman law

$$F = \sigma \epsilon T^4,$$

where

F = Total flux of energy (cals cm^{-2} mm^{-1})

σ = Universal constant ($8\ 312 \times 10^{-11}$ cal cm^{-2} $°K^{-4}$)

ϵ = Emissivity of the source

T = Temperature of the source (°K)

The flux of energy from the target is influenced by the atmospheric medium through which it passes to reach the sensor.

It can be seen from Fig. (6) that the absorption spectra of water vapor, carbon dioxide and ozone extends into the spectral range of the radiometer and therefore the radiometer will be sensitive to their effects. Of these, the effect of ozone in the 9.5μ wavelength region can be neglected since the bulk of the ozone in the atmosphere is confined to an altitude above 24 kms. Carbon dioxide has an absorption band extending from 12.7μ to 17μ. The peak absorption at 15μ is well outside the spectral response of the radiometer. Besides, the concentration by volume of carbon dioxide in the atmosphere is fairly constant at about 0.03 percent. Therefore the effect of carbon dioxide on the radiative flux can be estimated to a reasonable accuracy. Within the spectral interval of the radiometer this gas will contribute less than 2 percent of the total energy involved.

The effects of water vapor cannot be so easily dealt with since its concentration in the atmosphere varies with time and space.

However, it is possible to calculate the effects of water vapor on radiometric temperatures in an atmosphere with a known water vapor distribution. Once this is determined for various atmospheres with different water-vapor concentrations, it should be possible to correct an observed radiometric temperature under similar if not identical conditions.

On this basis, the following method has been developed to compute the effects of water vapor and carbon dioxide on radiometric temperature measurements.

III. THEORETICAL BASIS FOR CORRECTION TECHNIQUES

The radiant energy per unit area per unit time emitted by a target is modified as it passes through the atmosphere. For a medium of known water vapor concentration, the change in energy can be represented as shown in Fig. (8). This gives the percentage reduction of energy over a distance of 3,000 feet in an atmosphere with a total water vapor content of 1 gram per square centimeter. In this case, the energy is reduced to almost 60 percent of the total emitted by the target.

In order to estimate the loss of energy due to the absorption by carbon dioxide and water vapor, we assume an atmosphere with known vertical distribution of the pertinent radiating gases. We also assume

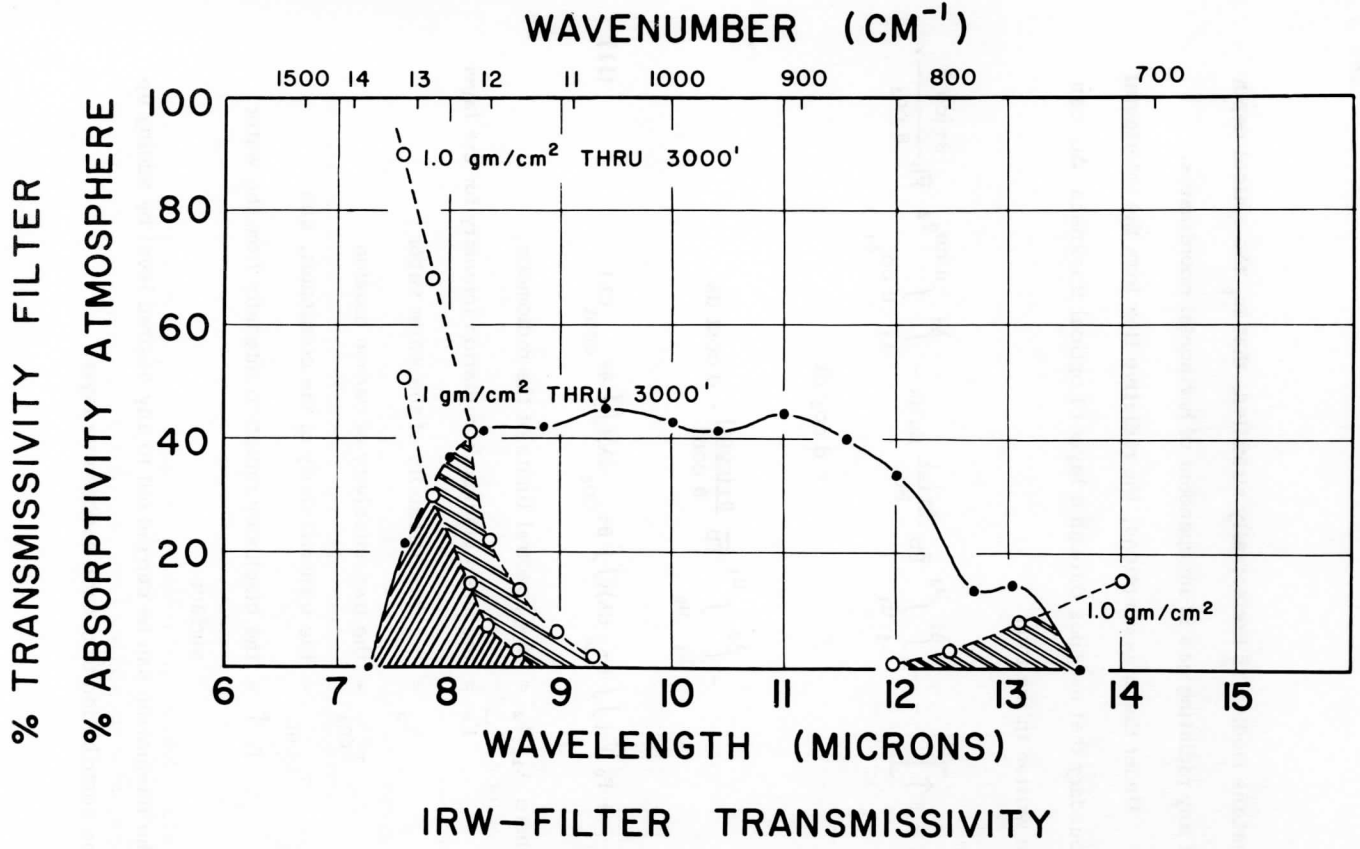

Figure 8. IRW-Filter Transmissivity.

that the medium is horizontally stratified, that is, the optical depth of any radiating gas is independent of horizontal coordinates.

Under these assumptions, the radiative flux from the interfacial boundary that escapes through a layer of optical thickness Δu can be written in the form

$$F\uparrow\Big]_{\lambda_1}^{\lambda_2} = -\int_{\lambda_1}^{\lambda_2}\int_{u_1}^{u_2} \bar{F}b\,\frac{\partial\tau(u)}{\partial u}\,du\,d\lambda - \int_{\lambda_1}^{\lambda_2}\int_{u\,co_{2_1}}^{u\,co_{2_2}} \bar{F}b\,\frac{\partial\tau(co_2)}{\partial\,co_2}\cdot$$

$$\cdot\, d\,co_2\,d\lambda$$

$$-\int_{\lambda_1}^{\lambda_2}\int_{u_0}^{u_1} \bar{F}b\,\frac{\partial\tau(cont)}{\partial\,cont}\cdot d\,cont\,d\lambda$$

$$+ F_0\uparrow\,(\int\int \partial\tau_\omega\,d\lambda)(\int\int \partial\tau_{co_2}\,d\lambda)(\int\int \partial\tau_{cont}\,d\lambda) \qquad (11)$$

where λ_1, λ_2 = the spectral limits of the radiometer,

$\bar{F}b$ = the mean blackbody radiation intensity for the layer

τ_u = the transmissivity of the water vapor

τ_{co_2} = the transmissivity of carbon dioxide

$\tau_{cont.}$ = the transmissivity of the continuum, and

$F_0\uparrow$ = the blackbody radiation intensity from the water surface.

The integration can be carried out to any desired level by adding up the contribution from each successive layer.

The irradiance so obtained for each layer can be converted into the equivalent blackbody temperature with the help of the calibration data for the instrument, Fig. (9). This was computed from the known physical characteristics of the radiometer, namely its filter function and the field of view.

In the absence of an interfering medium, the radiometer would read the same apparent temperature of the target from any altitude. However, the water vapor and carbon dioxide in the atmosphere interacts with the emitted target radiation resulting in a reduction in its intensity. This causes the radiometer to read a lower temperature with altitude. Hence, if the decrease in temperature of a target with altitude is known from computations, this change can be used to correct other radiometric measurements conducted from the same level and under similar atmospheric conditions.

By extending the computation to any desired level, a correction factor for that particular level can be obtained. In a practical case, when temperature surveys are conducted over a specified area over a period of time, a correction table applicable to the area and time can be prepared from a knowledge of the type of air masses that are likely to be present over the area. In such a case, from a general knowledge of the type of air mass influencing the surveyed area at a particular time, the correction table for that specific air mass can be referred to and the observed radiometric temperature corrected to within ± 0.5°C.

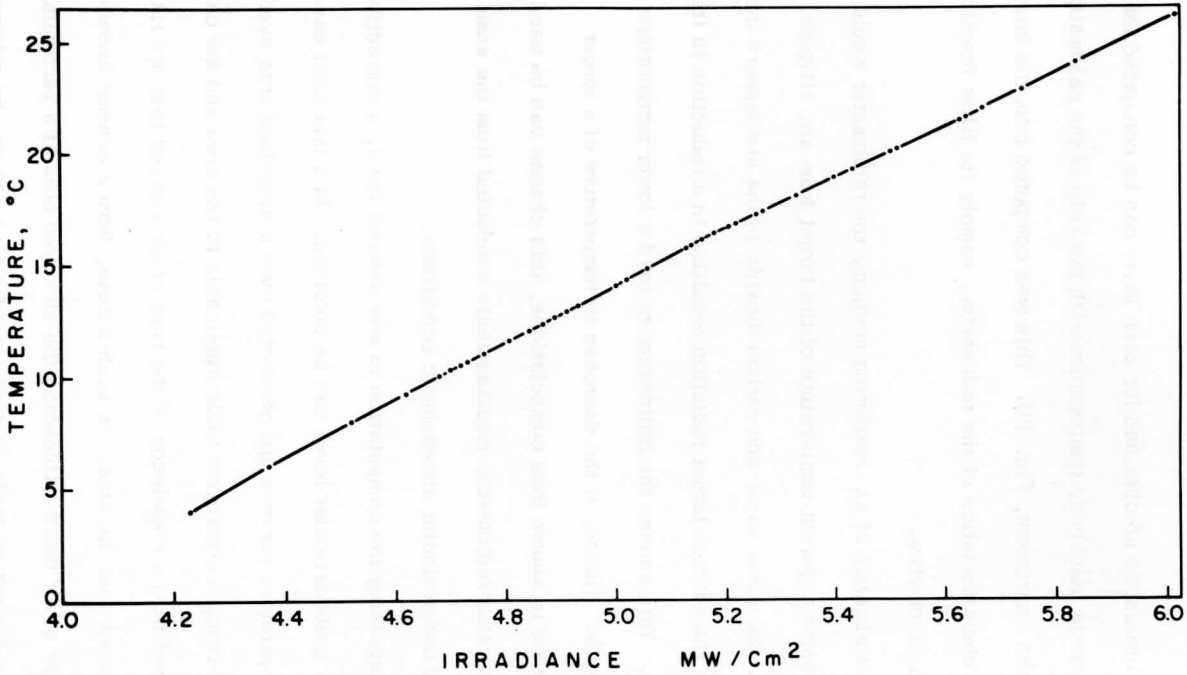

Figure 9. Computed Calibration, Irradiance vs Temperature

This will amount to making a correction table on the basis of air mass climatology.

IV. OBSERVATIONAL TECHNIQUES

A twin-engine aircraft provided by the Research Aviation Facility of the National Center for Atmospheric Research, Boulder, Colorado, was used to conduct an experimental sounding over Lake Superior with a Barnes IT-2 radiometer. The radiometer was flown after sunset on 20 July 1965 over a 25 mile track on a bearing of 140 degrees true out of Two Harbors, Minnesota, at the western end of Lake Superior. Repeated runs over the fixed track were undertaken from altitudes ranging from 1000 feet to 10,000 feet above the lake surface at one thousand foot intervals.

The radiometer sensing head was placed in a special rack fixed to the floor of the aircraft in such a way that an unobstructed vertical view of the target was possible through a port in the fuselage.

The output signal from the radiometer was recorded continuously along the flight track on a Westronics recording potentiometer. Using the calibration data for the radiometer and recording system obtained in the laboratory, the apparent temperature of the water surface along the track was determined. Results are shown in Fig. (10).

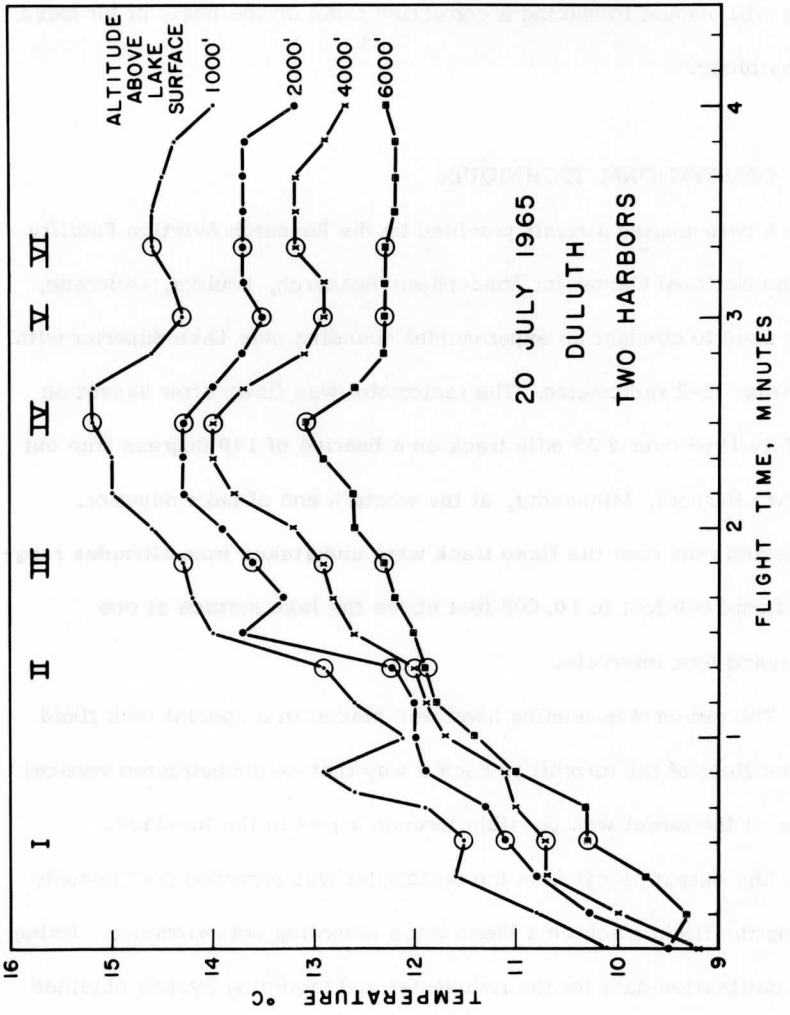

Figure 10. Barnes I. R. T.-2 Readings over the same track from different altitudes.

V. RESULTS

There is a steady decrease in the observed apparent surface temperature with altitude up to about 6000 feet. However, the temperature gradients were strikingly synchronous over the track from altitudes 1000 ft to 6000 ft. The next higher reading at 8000 ft shows an increase in the radiometric temperature. The air temperature also shows an inversion between 7000 and 8000 ft. A thin discontinuous stratiform cloud layer around 7000 ft was probably responsible for the increase in the radiometric temperature. It is of interest that visual sighting of the cloud could be made only after the radiometer anomaly was detected by the observer.

The liquid water droplets in the clouds are strong absorbers of the infrared radiation. A sufficiently thick cloud does not transmit any radiation incident upon it. The re-emission from the cloud is a function of the fourth power of its absolute temperature. If the cloud is thin, it partly transmits and partly emits, the sum of the two being equal to the incident radiation neglecting any reflected components. If the temperature of the cloud is higher (as shown by the inversion), then the emitted radiation will also be greater and this will cause the radiometer to record a higher reading.

With increasing altitude, the radiation from a larger surface area will reach the radiometer. Consequently the temperature pattern

obtained from 6000 ft lacks the finer details that were observed from 1000 ft. However there is good qualitative agreement between the temperature pattern obtained from a thousand ft and that from 4000 ft. This indicates that flights at higher levels than normally used (500 to 1500 ft) can provide useful information regarding the temperature pattern of the lake surface, the only restriction being that the intervening medium should have a low water vapor content. In some oceanographic work, an uncertainty in temperature of the order of a degree or less is important, in which case the observed temperature change with altitude would not be acceptable. At the same time, the technique has proved highly satisfactory for surface temperature surveys where gradients of several degrees celsius are common (Ragotzkie & Bratnick, 1965).

Change of apparent surface temperature with altitude ($\Delta T/\Delta z$) also varies along the flight track as shown in Fig. (11). Curves I through VI were plotted from data corresponding to six different locations along the track. It can be seen that the slope is not the same for all the curves with the result the net difference in temperature between the top and bottom layers ranged from one to three degrees, with an average difference of about two degrees.

The horizontal variation of apparent surface temperature change (ΔT) for each level is shown in Fig. (12). The mean temperature difference with height increased from 0.71 to 2000 ft to two degrees

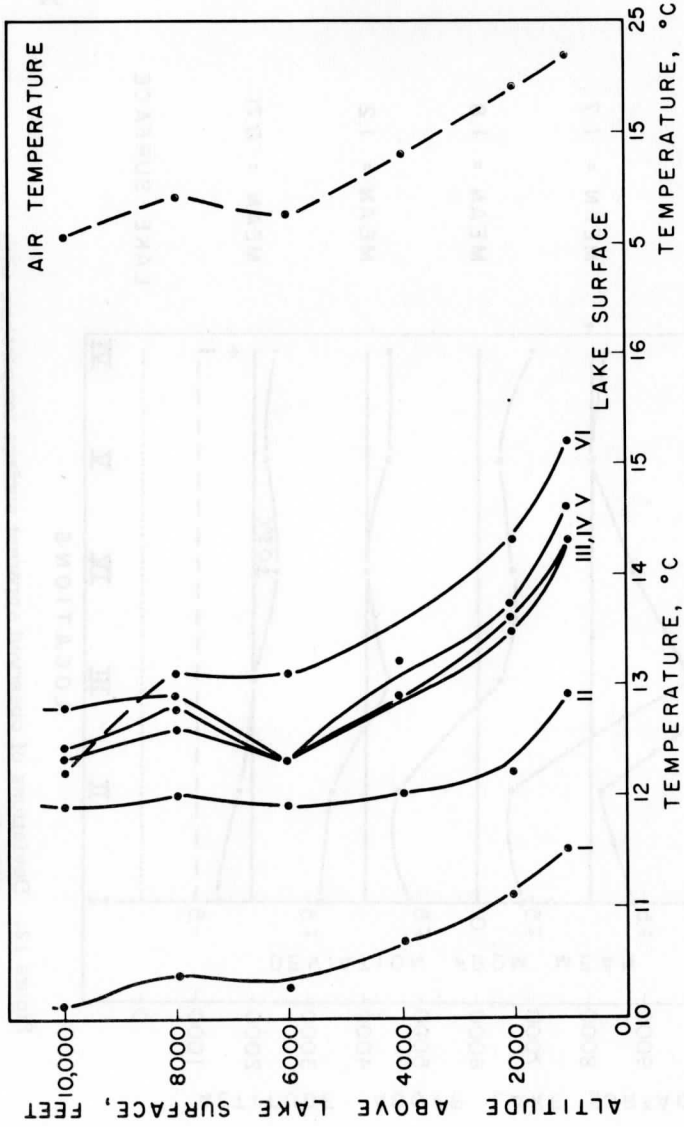

Figure 11. Observed target temperature at selected points on flight track from different altitudes.

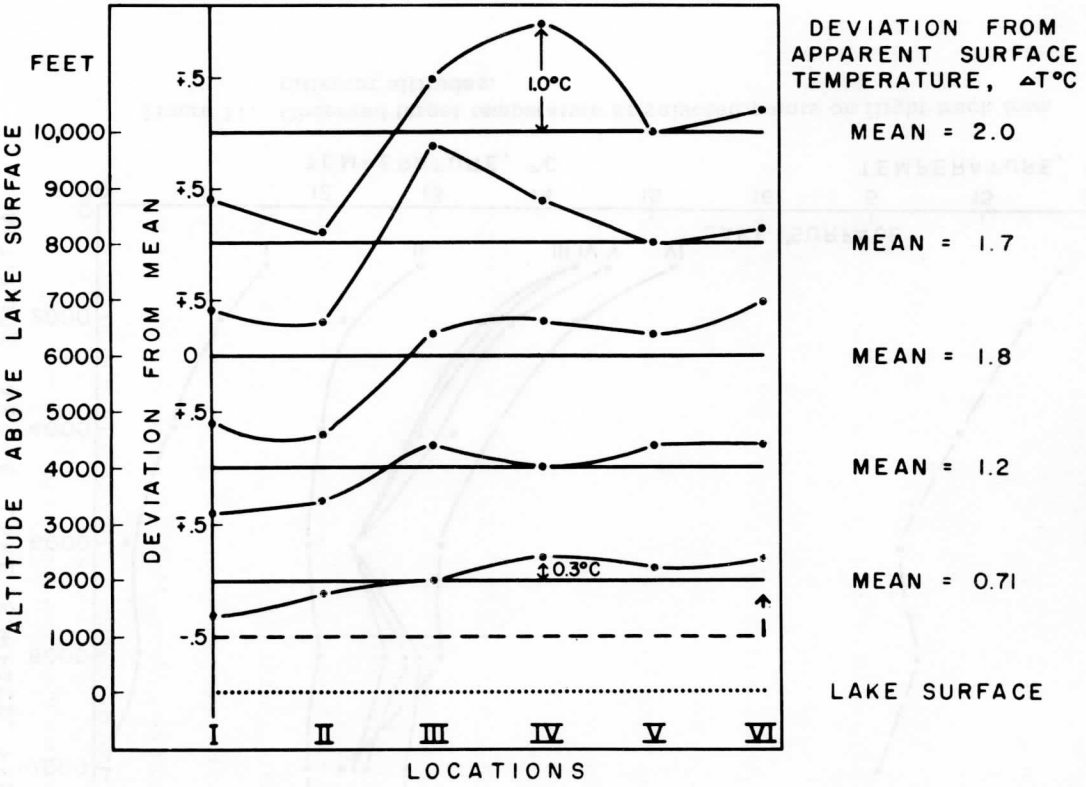

Figure 12. Deviations of observed apparent surface temperature with altitude.

at 10,000 ft. The range of variation about the mean value at a particular level also increased with increasing altitude from 0.3°C at 2000 ft to 1.0°C at 10,000 ft. However, the important result observed was the decrease in the apparent surface temperature with altitude which shows that the "wings" of the I.R.T. "window" can play a significant role under certain conditions. At the same time it may be pointed out that the filter characteristics of the instrument were designed to reduce the error caused by the absorption in the wings of the band. However this proved inadequate in eliminating the error completely since the contribution from the atmospheric constituents increased many times in these very same regions.

V. COMPARISON OF THEORY AND OBSERVATIONAL RESULTS

The method outlined in Chapter III for correcting radiometric temperatures was applied to the data obtained from the experimental flight on 20 July. The upward irradiance was computed according to Eq. (11). In the absence of upper air data near Two Harbors, humidity and air temperature data from the nearest upper air station at Sault Ste. Marie, Michigan, at the eastern end of Lake Superior was used to compute the flux density at each level. From the equivalent blackbody temperature, the correction factor for each level was determined.

For applying the correction, the temperature profiles on three locations in the flight track (Curves III and IV inFig. (11)) which have varying slopes were chosen. Figures (13) and (14) show the corrected profiles as against the observed. The observed data seems to be undercorrected at the lower levels (below 4000 ft) and overcorrected at the higher levels. To estimate the temperature of the water surface, the corrected profile is assumed to deviate equally on either side of the actual value as shown by the vertical lines in Figs. (13) and (14). The temperatures estimated from 4000 and 6000 ft agree well within 0.5°C. Also the estimated surface temperatures differ from that observed from 1000 ft by 0.1 to 0.4°C, which are well within the expected values. No attempt was made to extend the corrections higher than 6000 ft since the computed values could not be compensated for the effects of the observed cloud layer above that level.

The corrected temperature profile agrees with the theoretical predictions to within $\pm$ 0.5°C at 6000 ft. The absence of complete agreement may be attributed to the fact that the computations were based on humidity data obtained from the nearest upper air station at Sault Ste. Marie, 350 miles east of Two Harbors. Even if the same type of air mass existed over the two stations at that time, it is improbable that the characteristics of the air mass, especially its water vapor content, would be identical over the two places. A discrepancy between the predicted and the observed correction values

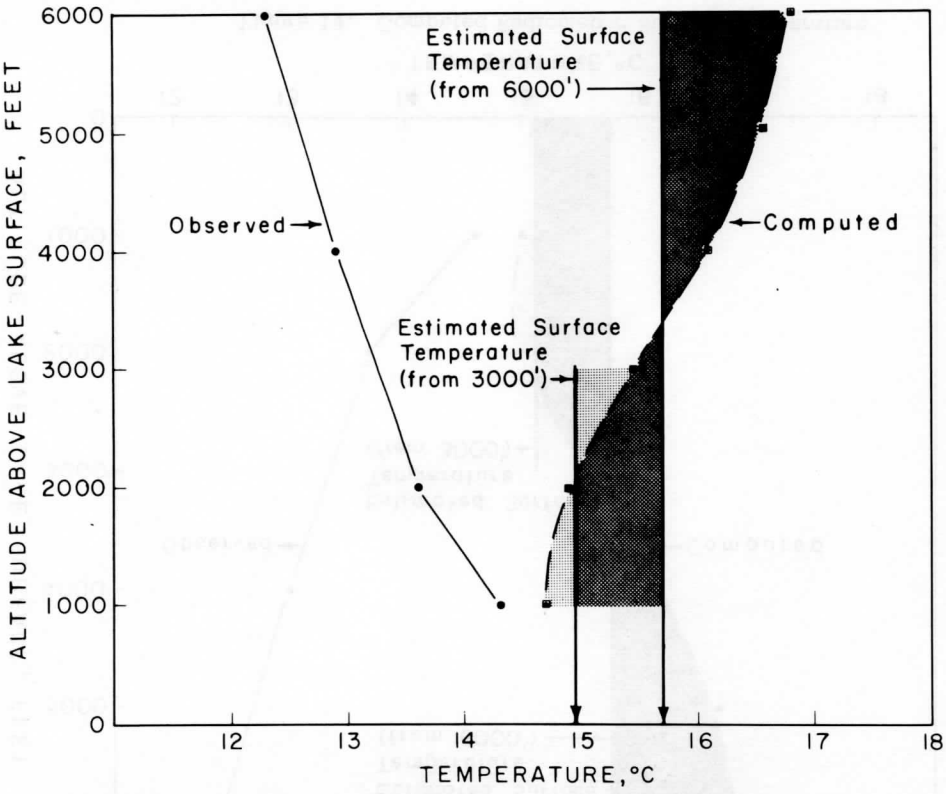

Figure 13. Computed Radiometric Surface Temperature

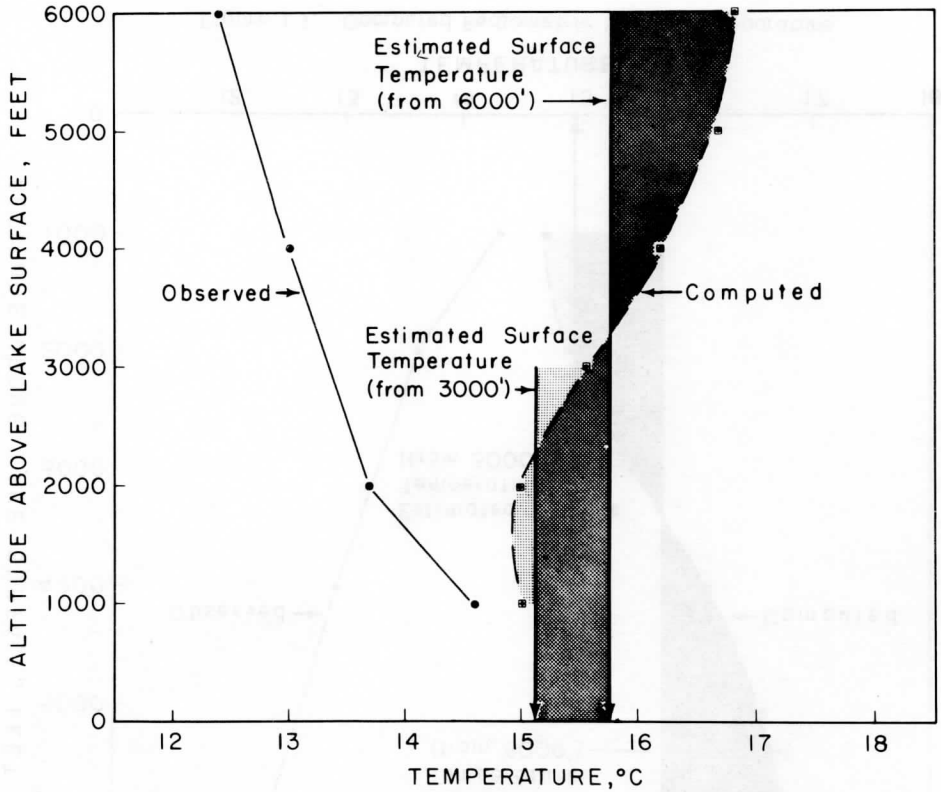

Figure 14. Computed Radiometric Surface Temperature

on this account was exptected.

Secondly, there is the strong probability of a surface inversion (of air temperature) being present in the first few meters above the cold water surface of the lake which is not detectable by a radiosonde observation. Therefore the computations will not incorporate the effects of this inversion whereas the radiometric reading will be affected by it.

Besides, as can be seen from Fig.(12), the observed surface temperature difference [ΔT] between any two levels (Tsfc (from 1000') - T sfc (from 2000', 4000' etc), vary substantially along the flight track of about 20 miles. At 10,000 ft, ΔT varies as much as $\pm$ 1.0°C about a mean value of 2.0°C. This shows that for any flight level, a single correction factor will not be adequate to correct all the points along the track.

Further, the increasing range of the horizontal fluctuations with altitude shows that the error is cumulative. Since these variations are not synchronous from level to level, it would appear that the humidity variation is not only a function of altitude but is also a significant variable along the horizontal direction. Therefore the usual assumption that the horizontal variation of water vapor can be neglected can no longer be considered valid.

CONCLUSIONS

The investigation has shown that with regard to the apparent surface temperature measurements using the Barnes Infrared Thermometer, Model IT-2, the effects of atmospheric interference in the wings of the spectral band are not negligible even when there are no visible clouds present. Observations show that the radiometric temperature of the target surface decreased steadily with altitude. For the same thickness of the medium, the decrease in temperature was also found to vary along the 20 mile flight track.

This indicated that the percentage by volume of the principal radiating constituent of the atmosphere varied not only as a function of altitude but also within short distances in the horizontal. This means that the observations along a flight track extending even a few miles cannot be corrected with the same accuracy using a single correction factor.

Despite these factors, the following conclusions can be stated:

1. Corrections based on a single upper air sounding reduced the error of the observed radiometric readings from 6000 ft to within $\pm$ 0.5°C. In the normal case for an uncorrected observation, an accuracy of this range is expected only from an altitude of a thousand feet above the target surface.

2. For radiometric surface temperature measurements from altitudes up to 10,000 ft or higher, the correction technique may prove valuable in

reducing the error range to within $\pm$ 1.0°C, provided the intervening medium is free from clouds of all types.

3. The discrepancy between the predicted and the observed correction figures may be narrowed down further if the distribution of water vapor concentration in the first 100 meters above the lake surface is known. It may also be helpful to consider smaller optical thicknesses of the medium for computing the upward flux, especially in regions where sharp humidity gradients are detected.

4. The fact that the observed decrease in surface temperatures in the first 1000 ft above the lake surface showed a positive correlation with the temperatures of the water indicates that the surface inversion of air temperature play a significant role in the radiometric temperature measurements. This also shows that it is the "temperature difference" rather than the temperature of either media that is more important in measurements using infrared techniques.

5. The correction technique was successfully applied to the temperate regions where the air mass in general has a low water vapor content. Further work is in progress to explore the feasibility of extending the technique to areas with different air mass characteristics such as the humid tropics.

PART III. POTENTIAL APPLICATIONS OF INFRARED AND MICROWAVE MEASUREMENTS

I. INTRODUCTION

Remote sensing by infrared and microwave techniques has found widespread application in a variety of fields ranging from meteorology and astronomy to hydrology, geography, ecology and agriculture. The basic requirement of all these applications is the sensing of radiation emitted by the respective radiators in specific wavelength regions. The signals obtained are then related to the particular property of the target one wants to measure.

The part of the electromagnetic spectrum that is of primary interest for this type of remote sensing techniques is that between 0.8 and 10,000 microns. Tables 3 and 4 (Kellogg, et al., 1964) lists some of the potentially usable regions of the spectrum for thermal and other measurements. Of these

(a) the visible spectrum, 0.3 to 0.8 microns, is principally used in remote sensing by photography.

(b) the 4 micron window is ideally suited for discovering sources with temperatures near 1000°K, such as forest fires and volcanoes.

(c) the 6.3 micron region is characterized by strong water vapor emission. Even though temperature dependence of water vapor signal is high, evaluation of apparent temperature in terms of true temperature and water vapor content seems difficult.

TABLE 3

LIST OF USABLE REGIONS OF THE SPECTRUM FOR THERMAL AND OTHER MEASUREMENTS

λ	Source[1]	Objective[2]	T-Power[3]	ε or ρ Varies[4]
0.8--3μ	Sun	Reflection by leaves, clouds, sea, etc.	---	20/1
4μ	Sea	Heat flow	10	?
6.3μ	H_2O	T of H_2O-vapor	6	Bands
8--12μ	Clouds, surfaces	T of surfaces	4	20%
15μ	CO_2	T of CO_2	4	Bands
20μ	Surfaces	T of surfaces	2	20%
0.8 cm	O_2	Amount of O_2 above clouds	1	Bands
1.3 cm	H_2O	Amount of H_2O-vapor	1	Bands
1.6 cm	Rain	Raininess	1	2/1
3 cm	Sea	Ice, icebergs	1	2/1
>10 cm	Discharges	Lightnings	---	---

[1] Source: Main origin of signals to satellite at wavelength λ. Term H_2O means water vapor.

[2] Objective: Reconnaissance to be gained from data. T = temperature in ^{o}K.

[3] T-Power: Power of T corresponding to the Planckian (B) at this λ and where T = 300^{o}K, e.g., $B(4\mu) \sim T^{10}$.

[4] ε or ρ Varies: Amount of variance observed for different target types.

(After Kellogg)

TABLE 4

THE INFRARED AND MICROWAVE AREAS

Name	Near IR	Intermediate IR	Far IR	Microwave IR
λ	0.8--3	3μ--50μ	50--$10^3\mu$	10^3--$10^5\mu$
ν	12,500--3300	3300--200	200--10	10--0.1 cm^{-1}
Separation	Prism	Prism	Grating	Tuning
Receiver[1]	Photoelectric cell	Cryogenic photoconductive cell →		←Microwave receiver
Molecular motions	Low electronic levels	Molecular vibration	←Molecular rotation→	
Main emitter[2]	Sun	Earth (heat)	Earth (heat)	Earth (heat)
Main atmospheric interference	H_2O, clouds	H_2O, CO_2, O_3 clouds	H_2O, clouds	H_2O, O_2, clouds (varying degree), rain
Emissivity of water	High	Very high	Decreasing	Very low
Snow and clouds	White	Black	?	Transparent
T vs. ϵ[3]	$T \gg \epsilon$	$T \sim \epsilon$	$T < \epsilon$	$T \ll \epsilon$

[1] All areas can be received with heat-sensing devices.

[2] Signals from lightning, radio stars, etc., are called discharge microwaves.

[3] Importance of terrestrial temperature variations compared to importance of emissivity variations.

(d) In the 8-13 micron atmospheric window, apparent temperatures are readily measured. Variations of apparent temperatures are caused by variations of (i) true surface temperature, (ii) surface emissivity and (iii) interference by atmospheric constituents. The variation due to atmospheric interference can be eliminated to a large extent by restricting the band to 10 to 11 microns. Even though this involves a reduction in the available energy, improved instrumentation techniques can minimize this defect.

(e) The 18 μ CO_2 emission band has been successfully used to measure effective stratosphere temperature.

(f) The 20 μ band could possibly be used for further studies of sea surface temperature. Here water has an emissivity of 0.94 and ice 0.98 for emission normal to the surface.

(g) In the 15-1000 μ band, liquid water surface changes from a black body to a reflector. The relation of signal strength to temperature shrinks to a simple proportionality factor. Atmospheric interference decreases to insignificant levels making it possible to detect small temperature variations.

(h) In the microwave region of 0.1 cm to 3 cm, atmospheric interference is limited to rain clouds. Absorption and scattering at 0.5 and 1.3 cm water band is sufficiently strong to allow rain reconnaisance possible, preferably by active techniques.

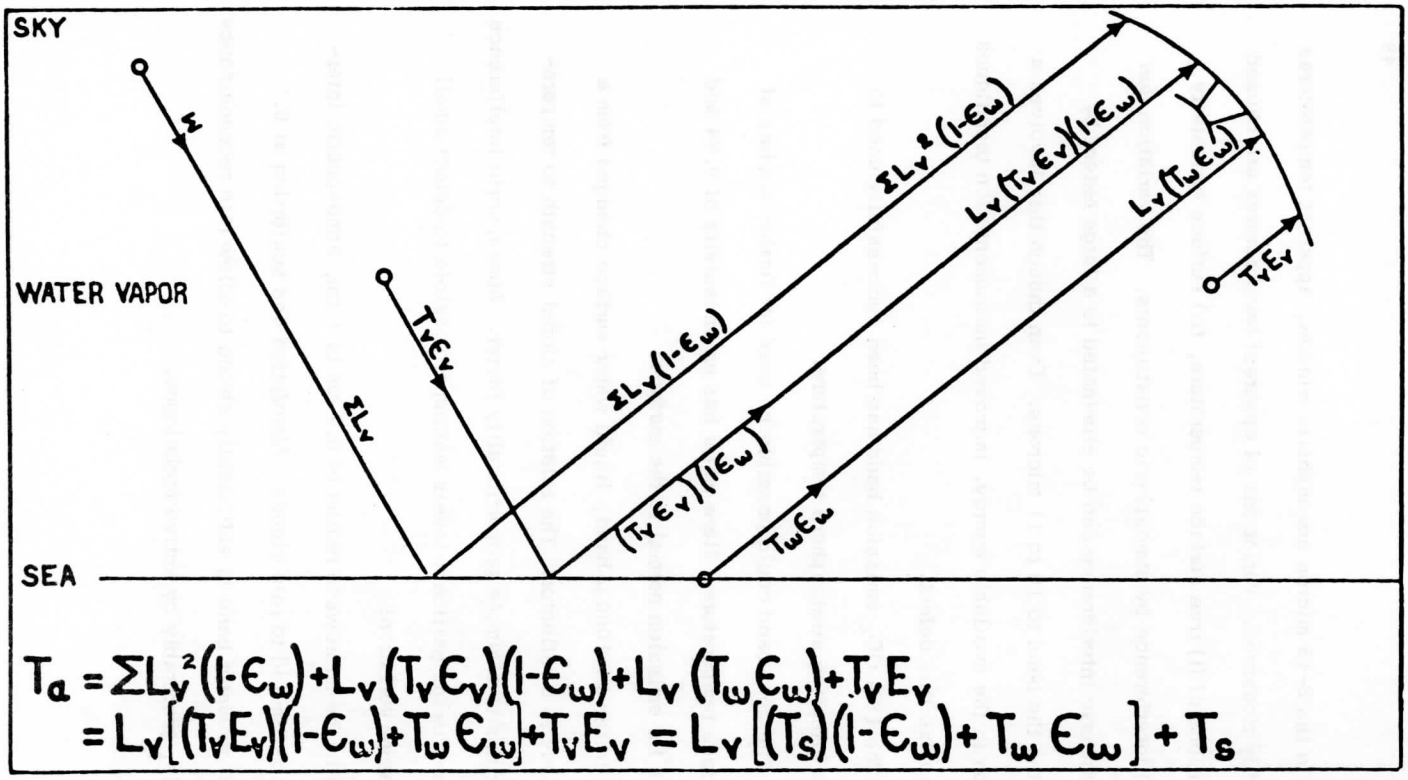

Figure 15. Schematic representation of sky, water vapor and sea contributions to apparent temperature (after Mardon).

At these wavelengths, the interfacial boundary or the "surface skin" ceases to be the radiating source. Radiations now originate from below the surface, the depth being a function of the wavelength. Hence measurement of apparent temperatures at different wavelengths can theoretically provide a vertical sounding of the top few centimeters of the water. This could be augmented with data from the surface skin using the 10 micron window.

(i) Beyond 2-3 cms, all atmospheric influence ceases. For sea water, apparent surface temperature can still be evaluated, provided surface roughness and its influence are known.

II. MEASUREMENT OF APPARENT SURFACE TEMPERATURE OF NATURAL WATER BODIES

The apparent temperature, Ta, measured by a radiometer is made up of

(i) a radiation term which is the product of the thermometric temperature of the target (T^4 for $\lambda < 10^{-2}$ cm) and its emissivity,

(ii) an emission term to account for the re-radiation by water vapor between the sensor and radiating source,

(iii) a reflectivity term which is the product of the apparent temperature of sky and the reflectivity of the water surface,

(iv) a term which involves the absolute temperature of the zenity sky (nearly 0° absolute) modified by the reflectivity of the water surface and the atmospheric losses.

The geometry of the general case can be represented as shown in Fig. (16). The apparent temperature Ta can now be written as the sum of the components in the form,

$$Ta \equiv T_w \epsilon_w L_v + T_v \epsilon_v + T_v \epsilon_v (1 - \epsilon_w) L_v + \sum L_v^2 (1 - \epsilon_w) \qquad (12)$$

Where T is the apparent temperature with subscripts v and w referring to water vapor and water respectively,

L_v is the loss term due to water vapor, related to zenith angle,

ϵ are the emissivities with subscripts v and w referring to water vapor and water, and

$\sum$ is the zenith sky temperature whose contribution is negligible compared to the other quantities.

$T_v \epsilon_v$ is essentially the apparent sky temperature (T_s) since the bulk of the atmospheric radiation originates from its water vapor content. Hence Eq. (12) can be rewritten as

$$Ta = [T_s(1 - \epsilon_w) + T_w \epsilon_w] L_v + T_s \qquad (13)$$

An identical expression for the apparent temperatures for wavelengths below 100 microns can be written in the form

$$Ta^4 = [Tv^4 \epsilon_v (1 - \epsilon_w) + T_w^4 \epsilon_w] L_v + Tv^4 \epsilon_v \qquad (14)$$

the radiation now being a function of the fourth power of the temperature of the radiator. Hence it can be seen that for the infrared region, the effects of the variation in emissivity of the water surface is much larger than at longer wavelengths. Similarly absorption and scattering by the

gases in the medium such as water vapor, carbon dioxide, nitrous oxide, oxygen, ozone, methane, and carbon monoxide (in decreasing order of importance) is also greater in the case of the infrared.

By operating in the "window region" of 8 to 14 microns, most of the atmospheric interference effects can be reduced to a minimum. However the contribution due to absorption by water vapor is significant even within the window region and the method outlined in Part II may be employed to minimize this error. The latter technique requires a knowledge of the relative humidity and temperature of the intervening atmosphere and since this information is not readily available on a global basis, the accuracy of the infrared measurements will also be restricted.

III. MEASUREMENTS OF TEMPERATURE GRADIENTS

In many oceanographic applications, temperature gradient data are as useful as the absolute values. Radiometric measurements can give reliable gradients over significant areas provided the parameters that contribute to errors in measurement do not change rapidly over the area. This stipulation, however, is not always met even over relatively short distances as described in Part II.

Also, regions of rapid change in the pertinent parameters and of erroneous gradients are also likely to be the regions of air mass boundaries which means there is a high probability of cloud cover

being present and this will automatically restrict the use of infrared techniques. Microwave measurements on the other hand are inherently capable of giving more accurate temperature gradients since the problem of atmospheric interference is far less serious at these wavelengths.

Within the areas where the horizontal gradients of the radiometric surface temperature are reliable, a single surface observation may provide a bench mark for calibration purposes. Additional information in the form of air temperature, relative humidity, wind speed and direction are helpful for a better evaluation of the observed data.

IV. MEASUREMENT OF HEAT FLUX ACROSS THE INTERFACIAL BOUNDARY

The solar radiation incident on the ocean surface is initially absorbed in the top few meters. Long wave radiation emitted from the surface of the water and absorbed by the atmospheric gaseous medium provides one way to supply energy to the atmospheric heat engine. The other processes by which the ocean loses heat to the atmosphere are evaporation, reflection and conduction of sensible heat. It seems these processes originate at different depths below the surface skin layer. Ewing (1964) quotes the following values for the different processes.

Evaporation	depth 3 Å
Reflection	5 Å
Radiation	10^6 Å

Heat loss due to radiation is a function of the temperature of the layer. Infrared measurements in the 8 to 14 micron band will give the temperature of the top layer within 0.02 cms from the interfacial boundary. If the transfer of heat by vertical convection in the upper 0.5 mm layer is small in comparison to conduction, the flow of heat between 0.5 mm depth and 0.05 mm depth is a measure of the total heat flow from the sea surface.

E. D. McAlister (1964) demonstrated through laboratory measurements that in the top 0.5 mm layer, heat transfer by convection is small compared to conduction. He therefore suggested a two wavelength infrared radiometer to measure the temperature gradient within the upper conduction layer (McAlister 1964). However the heat transfer values that he obtained using this technique were of uncertain accuracy because a reliable estimate of the effects of cloud cover could not be made. McAlister later disclosed the impracticability of using infrared techniques in view of the fact that "only 15% of the time does a 30 mile diameter circle on the earth's surface have 20% or less cloud cover"and infrared operation through cloud cover is of hardly any value for heat flux estimation from the water surface (McAlister, 1965). However, the possibility of operating under cloud cover with reasonable accuracy using aircraft should not be excluded. In the microwave region, this difficulty is inherently eliminated since radiation in the 0.1 to 3 cm waveband is not attenuated by cloud droplets.

The main problem that stands in the way of a two wavelength radiometric technique is the difficulty in estimating the exact depth from which radiation of a certain wavelength emanates.

When a plane electromagnetic wave in free space intersects a boundary of a medium having electrical properties appreciably different from free space, a portion of the energy is reflected while the balance enters the medium. The portion entering the medium undergoes an exponential decay according to the relation $\exp(-2aD)$ where D, called skin depth, is the reciprocal of the propagation constant and a, the absorption coefficient (Mardon, 1965).

Figure (17) shows skin depth D plotted as a function of average water temperature for three frequencies. By selecting the proper wavelengths, the water temperature as a function of depth in the top 4mm can be obtained. McAlister has shown recently that it is theoretically feasible to construct a two wavelength microwave radiometer that can measure the temperature gradient of the top conduction layer (McAlister, 1965). And since microwave radiation measurements seem to be possible through overcast sky conditions, the heat flux determination from sea surface seems to be possible under all but rainy conditions.

Several other applications of long wave radiometry in the fields of meteorology, geology, and oceanography are given below.

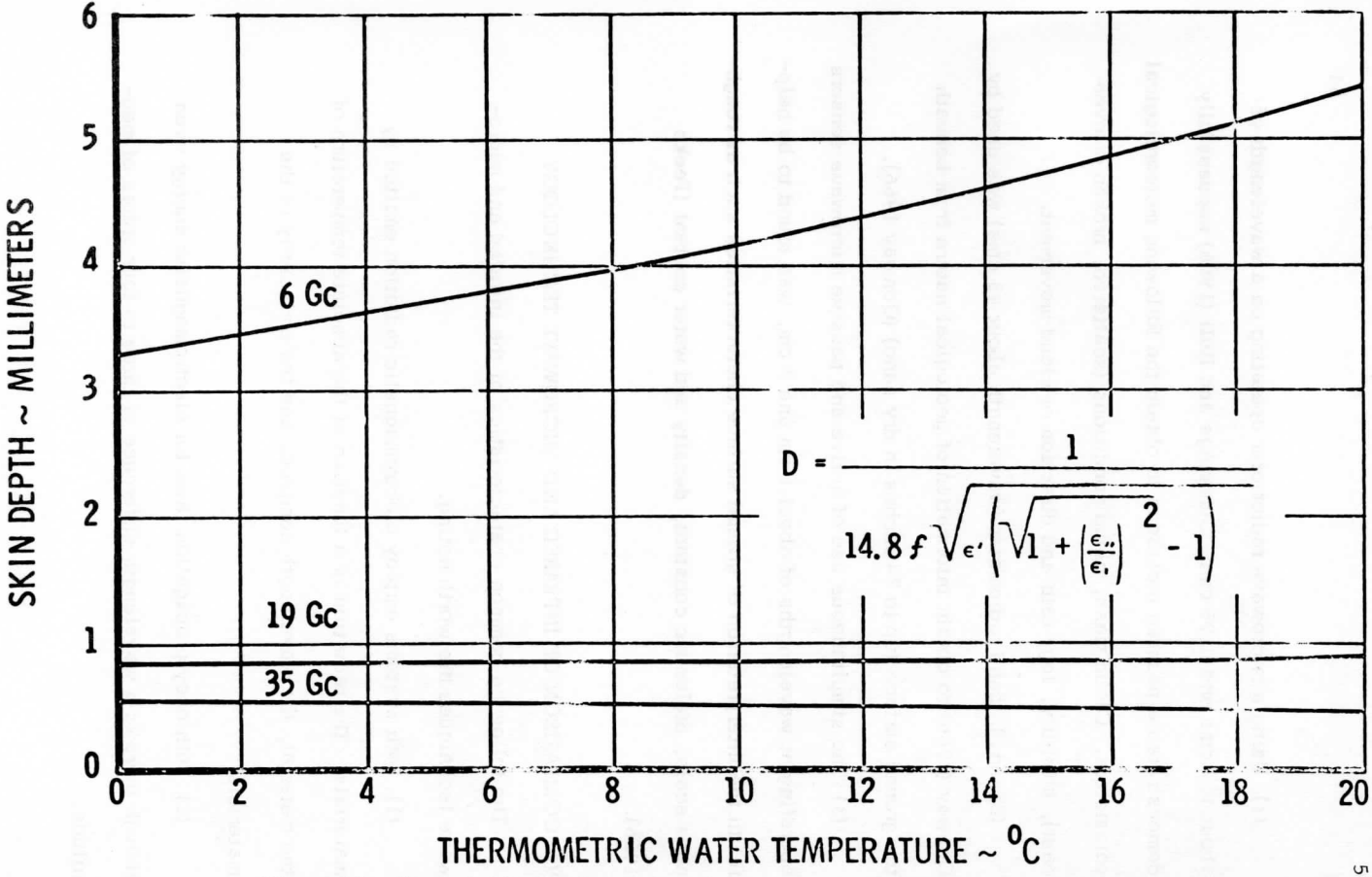

Figure 16. Plot of skin depth D as a function of average water temperature for three frequencies (after Mardon).

(1) Using a microwave radiometer operating on a wavelength of about 1.3 cms and 0.95 cms, Cummings and Hull (1966) successfully demonstrated a passive technique to obtain the following meteorological parameters. Cloud mass, cloud conditions (scattered, broken or overcast), humidity, fog, rain and direction of cloud movement.

(2) An L band radiometer (wavelength about 43 cms) was used by Conway (1966) to obtain information of geological nature from beneath the ground surface (up to 24 inches in dry sand) (Conway 1966).

(3) The simultaneous use of active and passive microwave sensors operating at wavelengths of about 1 cm and 3 cm, was found to be helpful in the interpretation of ground surface characteristics such as roughness scale, dielectric constant, density and water content (Peeke 1966).

V. COMPARISON OF INFRARED AND MICROWAVE TECHNOLOGY

The following common characteristics of the infrared and microwave techniques are worth noting.

(1) Both systems employ electromagnetic radiation emitted by materials. The radiation is a function of the absolute temperature of the material, the wavelength sampled, and the emissivity of the materials.

(2) Both obey propagation laws for electromagnetic energy even though there is a wavelength difference of three to four orders of magnitude.

(3) Each technique receives radiation as a random noise-like energy which must be integrated so that the signal is smoothed to reduce fluctuation peaks, the amount of soothing time being inversely related to the band width of the receiving system.

(4) The angular resolution of each system is dependent upon the aperture of the antenna or lens system used.

The chief differences between microwave and infrared techniques are:

(1) The attenuation due to the atmospheric constituents is much lower for microwave while infrared radiation has strong absorption hands due to gases like carbon dioxide, ozone and water vapor. A relatively clean window exists at 10-12 microns. For the microwave, at 1.8 cm wavelength, there is practically no atmospheric influence.

(2) The detector noise temperature is presently much lower for the microwave receivers than for the infrared. However, this factor offsets the naturally higher band widths available for the infrared detectors making the temperature resolution about equal for present state of the art equipment.

(3) The emission of electromagnetic energy from terrain objects is not entirely a surface phenomenon. As wavelength increases, the energy contribution of the underlying depths becomes significant, thus giving long wave radiometry the capability of determining conditions at depths of several centimeters in reasonably solid materials and meters for materials having a lower dielectric constant and or lower conductivity

(Kellogg 1964). Thus while infrared radiation can provide only the skin temperature, the longer wavelength radiation can give temperature information of layers beneath the surface.

VI. CONCLUSIONS

(1) Infrared techniques have already shown indications of being an important tool in the field of remote sensing, especially in skin temperature measurements.

(2) The one serious disadvantage of the technique is its unfavorable dependence on atmospheric constituents. On a global scale, the limitation put upon infrared techniques by cloud cover and by atmospheric attenuation are so serious that the alternative is to resort to longer wavelengths in the microwave band.

(3) Microwave technique holds interesting possibilities in many fields of remote sensing and has already shown promise of replacing infrared in such oceanographic measurements as heat flux through the air-sea interface (Staelin, 1965).

(4) The ability of infrared sensing devices to determine oceanographic parameters from satellites is limited by

a. the resolving power of the optical system that forms the image for the scanning system.

b. the minimum radiometric temperature differential that the infrared part of the system can sense.

c. the amount of cloud cover and other meteorological conditions.

(5) For the microwave system, the sensed temperature is strongly affected by the sea state because the water reflects approximately half the energy incident upon it. Reflection coefficient of sea depends on

a. the dielectric constant of sea water, a complex quantity which is a function of the frequency and temperature.

b. the electrical conductivity which is fairly high for salt water.

In conclusion, it may be pointed out that there are strong possibilities of using satellite-borne sensors for the measurement of heat flux through the surface of oceans, atmospheric temperature gradient and rainfall distribution. Few of these parameters have as yet been measured from the satellites because of the lack of proper instrumentation. The most promising tool seems to be the new passive microwave (0.5 to 10 cm) systems which permit the detection of thermal flux in a part of the spectrum where clouds are relatively transparent.

ACKNOWLEDGMENTS

The authors wish to express their appreciation to Dr. P. M. Kuhn and Dr. W. L. Smith for their helpful critiques and assistance in the computer programming of the radiative transfer equation. Aircraft support was provided by The Research Aviation Facility of the National Center for Atmospheric Research.

REFERENCES

1. Bell, E. E., 1959. Radiometric quantities, symbols and units. Proceedings I.R.E., 47: 1432-1434.

2. Berberian, G. A., A. H. Oshiver, J. R. Clark, R. B. Stone, 1965. Factors in the measurement of absolute surface temperature by infrared emissivity, Proc. Third Symposium on Remote Sensing, Univ. of Mich., Ann Arbor, Mich., 737-762.

3. Buettner, K., 1965. The consequence of terrestrial surface infrared emissivity, Proc. Third Symposium on Remote Sensing, Univ. of Mich., Ann Arbor, Mich., 549-562.

4. Collins Research Report, 1961. Passive microwave observation of terrain features, Collins Radio Co., Cedar Rapids, Iowa.

5. Conway, W. H., R. T. Sakamoto, 1965. Microwave radiometer measurement program, Proc. Third Symposium on Remote Sensing, Univ. of Mich., Ann Arbor, Mich., 339-356.

6. Cummings, C. A., and J. W. Hull, 1966. Microwave radiometric meteorological observations, Proc. Fourth Symposium on Remote Sensing, Univ. of Mich., Ann Arbor, Mich., 263-272.

7. Ewing, Gifford C., 1965. The outlook for oceanographic observations from satellites, Proc. Third Symposium on Remote Sensing, Univ. of Mich., Ann Arbor, Mich., 691-716.

8. Hess, S. L., 1959. Introduction to Theoretical Meteorology, Henry Holt and Company, New York.

9. Kellogg, W. W., 1964. Memorandum, NASA 21 (7), NASA.

10. Mardon, A., 1965. Application of microwave radiometers to oceanographic measurements, Proc. Third Symposium on Remote Sensing, Univ. of Mich., Ann Arbor, Mich., 763-779.

11. McAlister, E. D., 1964, Infrared-optical technique applied to oceanography, Applied Optics, 3(5): 609-612.

12. McAlister, E. D., 1965. A two wavelength microwave radiometer for measurement of the total heat exchange at the air-sea interface, Applied optics, 4 (1): 145-146.

13. Peake, W. H., R. L. Riegler, and C. H. Schultz, 1966. Proc. Fourth Symposium on Remote Sensing, Univ. of Mich., Ann Arbor, Mich., 771-778. The mutual interpretation of active and passive microwave sensor outputs.

14. Ragotzkie, R. A., M. Bratnick, 1965. Infrared temperature patterns on Lake Superior and inferred vertical motions, Great Lakes Research Division, 13, Univ. of Mich., 349-357.

15. Squire, J. S., Jr., 1965. Airborne oceanographic program of the Tiburen Marine Laboratory and some observations on future development and use of this technique, Oceanography from Space, The Woods Hole Oceanographic Institution, Woods Hole, Mass., 119-123.

16. Staelin, D. H., 1965. Microwave spectral measurement applicable to oceanography, Oceanography from Space, the Woods Hole Oceanographic Institution, Woods Hole, Mass., 229-234.

UNCLASSIFIED

Security Classification

DOCUMENT CONTROL DATA - R&D

(Security classification of title, body of abstract and indexing annotation must be entered when the overall report is classified)

1. ORIGINATING ACTIVITY *(Corporate author)*
Meteorology Department
University of Wisconsin
Madison, Wisconsin 53706

2a. REPORT SECURITY CLASSIFICATION
UNCLASSIFIED

2b. GROUP

3. REPORT TITLE
REMOTE SENSING BY INFRARED AND MICROWAVE RADIOMETRY

4. DESCRIPTIVE NOTES *(Type of report and inclusive dates)*

5. AUTHOR(S) *(Last name, first name, initial)*
Menon, Velayudh Krishna
Ragotzkie, Robert A.

6. REPORT DATE	7a. TOTAL NO. OF PAGES	7b. NO. OF REFS
February 1967	59	16

8a. CONTRACT OR GRANT NO.	9a. ORIGINATOR'S REPORT NUMBER(S)
Nonr 1202(07)	Technical Report No. 31.
b. PROJECT NO. NR 387-022	
c.	9b. OTHER REPORT NO(S) *(Any other numbers that may be assigned this report)*
d.	

10. AVAILABILITY/LIMITATION NOTICES
Distribution of this document is unlimited.

11. SUPPLEMENTARY NOTES	12. SPONSORING MILITARY ACTIVITY
	Geography Branch Office of Naval Research Washington, D. C.

13. ABSTRACT

In part I, the basic principles involved in the remote sensing by passive techniques in the infrared to microwave region of the electromagnetic spectrum are discussed. Whereas the radiation below ten micron wavelength has found distinct application in many fields, the region between 0.1 to 10 cms has a decided advantage in situations where the atmospheric constituents interfere. (U)

Part II deals with the specific problem of atmospheric interference in the 8 to 14 micron wavelength region due to water vapor and carbon dioxide. A technique for correcting radiometric measurements of surface temperatures for interference by these two constituents is suggested. (U)

Part III deals with the potential applications of infrared and microwave radiometry to the measurement of surface temperature of natural water bodies, horizontal temperature gradients, and the heat flux across the sea-air interface. The relative advantages of infrared and microwave techniques are compared. (U)

DD FORM 1 JAN 64 1473

UNCLASSIFIED

Security Classification

14. KEY WORDS	LINK A		LINK B		LINK C	
	ROLE	WT	ROLE	WT	ROLE	WT
remote sensing emissivity apparent temperature radiative transfer heat budget						

INSTRUCTIONS

1. ORIGINATING ACTIVITY: Enter the name and address of the contractor, subcontractor, grantee, Department of Defense activity or other organization *(corporate author)* issuing the report.

2a. REPORT SECURITY CLASSIFICATION: Enter the overall security classification of the report. Indicate whether "Restricted Data" is included. Marking is to be in accordance with appropriate security regulations.

2b. GROUP: Automatic downgrading is specified in DoD Directive 5200.10 and Armed Forces Industrial Manual. Enter the group number. Also, when applicable, show that optional markings have been used for Group 3 and Group 4 as authorized.

3. REPORT TITLE: Enter the complete report title in all capital letters. Titles in all cases should be unclassified. If a meaningful title cannot be selected without classification, show title classification in all capitals in parenthesis immediately following the title.

4. DESCRIPTIVE NOTES: If appropriate, enter the type of report, e.g., interim, progress, summary, annual, or final. Give the inclusive dates when a specific reporting period is covered.

5. AUTHOR(S): Enter the name(s) of author(s) as shown on or in the report. Enter last name, first name, middle initial. If military, show rank and branch of service. The name of the principal author is an absolute minimum requirement.

6. REPORT DATE: Enter the date of the report as day, month, year; or month, year. If more than one date appears on the report, use date of publication.

7a. TOTAL NUMBER OF PAGES: The total page count should follow normal pagination procedures, i.e., enter the number of pages containing information.

7b. NUMBER OF REFERENCES: Enter the total number of references cited in the report.

8a. CONTRACT OR GRANT NUMBER: If appropriate, enter the applicable number of the contract or grant under which the report was written.

8b, 8c, & 8d. PROJECT NUMBER: Enter the appropriate military department identification, such as project number, subproject number, system numbers, task number, etc.

9a. ORIGINATOR'S REPORT NUMBER(S): Enter the official report number by which the document will be identified and controlled by the originating activity. This number must be unique to this report.

9b. OTHER REPORT NUMBER(S): If the report has been assigned any other report numbers *(either by the originator or by the sponsor)*, also enter this number(s).

10. AVAILABILITY/LIMITATION NOTICES: Enter any limitations on further dissemination of the report, other than those imposed by security classification, using standard statements such as:

(1) "Qualified requesters may obtain copies of this report from DDC."

(2) "Foreign announcement and dissemination of this report by DDC is not authorized."

(3) "U. S. Government agencies may obtain copies of this report directly from DDC. Other qualified DDC users shall request through _____."

(4) "U. S. military agencies may obtain copies of this report directly from DDC. Other qualified users shall request through _____."

(5) "All distribution of this report is controlled. Qualified DDC users shall request through _____."

If the report has been furnished to the Office of Technical Services, Department of Commerce, for sale to the public, indicate this fact and enter the price, if known.

11. SUPPLEMENTARY NOTES: Use for additional explanatory notes.

12. SPONSORING MILITARY ACTIVITY: Enter the name of the departmental project office or laboratory sponsoring *(paying for)* the research and development. Include address.

13. ABSTRACT: Enter an abstract giving a brief and factual summary of the document indicative of the report, even though it may also appear elsewhere in the body of the technical report. If additional space is required, a continuation sheet shall be attached.

It is highly desirable that the abstract of classified reports be unclassified. Each paragraph of the abstract shall end with an indication of the military security classification of the information in the paragraph, represented as *(TS), (S), (C), or (U)*.

There is no limitation on the length of the abstract. However, the suggested length is from 150 to 225 words.

14. KEY WORDS: Key words are technically meaningful terms or short phrases that characterize a report and may be used as index entries for cataloging the report. Key words must be selected so that no security classification is required. Identifiers, such as equipment model designation, trade name, military project code name, geographic location, may be used as key words but will be followed by an indication of technical context. The assignment of links, roles, and weights is optional.

Chief of Naval Research
Attn Geography Branch
Office of Naval Research
Washington, D. C. 20360 2

Defense Documentation Center
Cameron Station
Alexandria, Virginia 22314 20

Director Naval Rsch Lab
Attn Tech Information Officer
Washington, D. C. 20360 6

Commanding Officer
New York Area Office
Office of Naval Research
207 West 24th Street
New York, New York 10011

Commanding Officer
Office of Naval Rsch Branch Office
219 So Dearborn
Chicago, Illinois 60601

Commanding Officer
Office of Naval Research
Branch Office, Box 39
Fleet Post Office
New York, New York 09510

Chief of Naval Operations/OP 922 H/
Department of the Navy
Washington, D. C. 20360

Chief of Naval Operations/OP 03 EG/
Department of the Navy
Washington, D. C. 20360

Chief of Naval Operations/OP 07T
Department of the Navy
Washington, D. C. 20360

Hdqs., U. S. Marine Corps
Rsch and Development Branch
Arlington Annex
Washington, D. C. 20360

The Oceanographer
U. S. Navy Oceanographic Office
Washington, D. C. 20360

Commanding Officer
U. S. Naval Reconnaissance & Technical
Support CTRE
4301 Suitland Road
Washington, D. C. 20360

Commanding General
U. S. Army Natick Laboratories
ATTN: AMXRE - EG
Natick, Massachusetts 01760

Chief of Naval Rsch/Code 111/
Office of Naval Research
Washington, D. C. 20360

Chief of Naval Rsch/Code 416/
Office of Naval Research
Washington, D. C. 20360

Chief of Naval Rsch/Code 461/
Office of Naval Research
Washington, D. C. 20360

Chief of Naval Operations/OP09B7/
Department of the Navy
Washington, D. C. 20360

Defense Intelligence Agency
DIAAP-IE4
Department of Defense
Washington, D. C. 20360

Chief, Bureau of Weapons
Meteorological Division
Department of the Navy
Washington, D. C. 20360

Directorate of Intelligence
Headquarters, U. S. Air Force
Washington, D. C. 20360

Commander
AF Cambridge Research Center
Attn Carlton E. Molineux
Terrestrial Sciences Lab
Bedford, Massachusetts

Arctic,Desert, Tropic
Information Center
Aerospace Studies Institute
Maxwell AFB, Alabama 36112

Headquarters Air Weather Service
Scott Air Force Base
Illinois

Commander Air Rsch & Dev
Attn Geophysics Division
Washington, D. C. 20360

Dr. Leonard S. Wilson
Office of Chief of Rsch & Dev
Washington, D. C. 20360

Directorate of Topography
& Military Engineering
Office Chief of Engineers
Gravelly Point
Washington, D. C. 20360

Waterways Experiment Station
Attn Geology Branch
U. S. Army Corps of Engineers
Vicksburg, Mississippi

U. S. Army Cold Regions Res & Eng Lab
P. O. Box 282
Hanover, New Hampshire

Central Intelligence Agency
Attn OCR/DD - Publications
Washington, D. C. 20505

Director
Office of Geography
Department of Interior
Washington, D. C. 20360

U. S. Weather Bureau
Attn Scientific Services Div
24th & M St. N.W.
Washington, D. C. 20360

Area Officer
Foreign Agricultural Service
U. S. Dept of Agriculture
Washington, D. C. 20360 2

Department of State
External Rsch Division
Room 8733
ATTN Chief, Government Branch
Washington, D. C. 20360 2

Dr. Paul A. Siple
Scientific Adviser
U. S. Army Research Office
Washington, D. C. 20360

Research Analysis Corporation
McLean, Virginia

Dr. Erhard M. Winkler
Department of Geology
University of Notre Dame
Notre Dame, Indiana

Dr. Richard J. Russell
Coastal Studies Institute
Louisiana State University
Baton Rouge, Louisiana 70803

Dr. Jonathan D. Sauer
Department of Botany
University of Wisconsin
Madison, Wisconsin 53706

Dr. John H. Vann
Dept of Geography & Geology
State University College
1300 Elmwood Avenue
Buffalo, New York

Dr. H. Homer Aschmann
Division of Social Science
University of California
Riverside, California 92502

Dr. Edward B. Espenshade
Department of Geography
Northwestern University
Evanston, Illinois 60201

Dr. John R. Mather
C. W. Thornthwaite Associates
Route #1, Centerton
Elmer, New Jersey 08318

Dr. Kirk H. Stone
Department of Geography
Univ of Georgia
Athens, Georgia 30601

Dr. David S. Simonett
Department of Geography
University of Kansas
Lawrence, Kansas 66044

Dr. James P. Latham
Prof & Chairman of Geography
Florida Atlantic Univ
Baco Raton, Florida 33432

Dr. Charles E. Olson
Department of Forestry
University of Illinois
Urbana, Illinois

Dr. William E. Benson
Program Director for Earth Sci
National Science Foundation
Washington, D. C. 20360

Dr. Frank Ahnert
Department of Geography
University of Maryland
College Park, Maryland 20740

Dr. Theo L. Hills
Geography Department
McGill University
Montreal, Quebec
Canada

Dr. Leslie Curry
Department of Geography
University of Toronto
Toronto, Ontario
Canada

Dr. M. Gordon Wolman
Department of Geography
Johns Hopkins University
Baltimore 18, Maryland

Dr. L. A. Peter Gosling
Dept of Geography
University of Michigan
Ann Arbor, Michigan

Dr. Thomas R. Smith
Department of Geography
University of Kansas
Lawrence, Kansas 66044

U. S. Naval Academy Library
U. S. Naval Academy
Annapolis, Maryland

Prof. Edward J. Taaffe
Department of Geography
The Ohio State University
1755 South College Road
Columbus, Ohio 43210

Dr. Sven Orvig
Department of Geography
McGill University
Montreal, Quebec
Canada

Library, Geological Survey of
Canada
Room 350
601 Booth Street
Ottawa 1, Ontario
Canada

National Research Council
Librarian
Ottawa, Ontario
Canada

Dr. J. Brian Bird
Dept of Geography
McGill University
Montreal, Quebec
Canada

Dr. Harry P. Bailey
Div of Social Sciences
University of California
Riverside, California 92502

Dr. F. R. Fosberg
Pacific Sciences Board
National Research Council
Washington, D. C. 20360

Prof. Harley J. Walker
Dept of Geography
Louisiana State University
Baton Rouge, Louisiana 70803

Dr. David H. Miller
Dept of Geography
University of Wisconsin
Milwaukee, Wisconsin

Dr. Warren C. Thompson
Dept Meteorology & Ocean
U. S. Naval Post Grad. School
Monterey, California 93940

Dr. John R. Borchert
Department of Geography
University of Minnesota
Minneapolis, Minnesota 55455

Dr. Robert M. Glendinning
Dept of Geography
University of California
Los Angeles, California 90024

Dr. Richard F. Logan
Dept of Geography
University of California
Los Angeles, California 90024

U. S. Fish & Wildlife Service
Dept of the Interior
Washington, D. C. 20360

Department of Geography
University of Washington
Seattle, Washington 98105

Dept of Meteorology and
Oceanography
Naval Postgraduate School
Monterey, California 93940

Director
Arctic Institute of North America
1619 New Hampshire Avenue, N.W.
Washington, D. C. 20009

Dr. Jack P. Ruina
Director Advanced Research
Projects Agency
Office of the Sec of Defense
The Pentagon
Washington, D. C. 20360

ONR Branch Office
219 So. Dearborn
Chicago, Illinois 60601

Robert E. Frost
U. S. Army Corps of Engineers
Cold Regions Research and
Engineering Laboratory
Hanover, New Hampshire

Dr. Charles C. Bates
Assistant Civilian Director
U. S. Naval Oceanographic Office
Washington, D. C. 20390